

## Electronic Supplementary Information

# New diclofenac salts with the dense hydrogen bond donor propane-1,3-diaminium

Jaxon R. Breckell,<sup>a</sup> Luke Conte,<sup>a</sup> Michael W. Potts,<sup>a</sup> Pradnya S. Sawant,<sup>b</sup> Raymond J. Butcher,<sup>c</sup> Beena K. Vernekar,<sup>\*b</sup> and Christopher Richardson<sup>\*a</sup>

<sup>a</sup> School of Chemistry and Molecular Bioscience Science, University of Wollongong, Wollongong NSW 2522, Australia

<sup>b</sup> Department of Chemistry, Government College of Arts, Science and Commerce, Khandola, Marcela, Goa, India

<sup>c</sup> Department of Chemistry, Howard University, Washington, DC 20059, USA

### Table of Contents

1.	A selection of reported Diclofenac salts.....	2
2.	Fourier Transform Infrared Spectroscopy .....	6
3.	NMR Spectroscopy .....	7
4.	Single Crystal X-ray Diffraction .....	20
5.	Powder X-Ray Diffraction .....	30
6.	TG-DSC Data .....	37
7.	ESI Mass Spectrometry .....	46

## 1. A selection of reported Diclofenac salts

**Table S 1** Table of selected organic salts of diclofenac.

Cation	CCDC	Reference
Acridinium	2211637	A. Mirocki, E. Conterosito, L. Palin, A. Sikorski, M. Milanesio, M. Lopresti, CCDC 2211637: Experimental Crystal Structure Determination, 2022, DOI: 10.5517/ccdc.csd.cc2d7d46
4-Aminopyridinium	1480982	P. K. Goswami, V. Kumar, A. Ramanan, <i>J. Mol. Struct.</i> , 2020, <b>1210</b> , 128066. <a href="https://doi.org/10.1016/j.molstruc.2020.128066">https://doi.org/10.1016/j.molstruc.2020.128066</a>
3-Aminopyridinium monohydrate	1480981	P. K. Goswami, V. Kumar, A. Ramanan, <i>J. Mol. Struct.</i> , 2020, <b>1210</b> , 128066. <a href="https://doi.org/10.1016/j.molstruc.2020.128066">https://doi.org/10.1016/j.molstruc.2020.128066</a>
3-Ammoniopyridinium	1480979	P. K. Goswami, V. Kumar, A. Ramanan, <i>J. Mol. Struct.</i> , 2020, <b>1210</b> , 128066. <a href="https://doi.org/10.1016/j.molstruc.2020.128066">https://doi.org/10.1016/j.molstruc.2020.128066</a>
2-Aminopyridinium	1480978	P. K. Goswami, V. Kumar, A. Ramanan, <i>J. Mol. Struct.</i> , 2020, <b>1210</b> , 128066. <a href="https://doi.org/10.1016/j.molstruc.2020.128066">https://doi.org/10.1016/j.molstruc.2020.128066</a>
Cytosinium	2180777	F. J. Acebedo-Martínez, C. Alarcón-Payer, H. M. Barrales-Ruiz, J. Niclós-Gutiérrez, A. Domínguez-Martín, D. Choquesillo-Lazarte, <i>Crystals</i> 2022, <b>12</b> , 1038. <a href="https://doi.org/10.3390/crust12081038">https://doi.org/10.3390/crust12081038</a>
L-proline	1584472 1863145	I. Nugrahani, D. Utami, S. Ibrahim, Y. P. Nugraha and H. Uekusa, <i>Eur. J. Pharm. Sci.</i> , 2018, <b>117</b> , 168–176. <a href="https://doi.org/10.1016/j.ejps.2018.02.020">https://doi.org/10.1016/j.ejps.2018.02.020</a>  A. O. Surov, A. P. Voronin, M. V. Vener, A. V. Churakov and G. L. Perlovich <i>CrystEngComm</i> , 2018, <b>20</b> , 6970-6981. <a href="https://doi.org/10.1039/C8CE01458B">https://doi.org/10.1039/C8CE01458B</a>
Berberine (B) B-dcfn·0.5CH <sub>2</sub> Cl <sub>2</sub> ·2H <sub>2</sub> O	1965859 1965858	W. Sun, L. Zuo, T. Zhao, Z. Zhu, and G. Shan <i>Acta Crystallogr., Sect..</i> 2019, <b>C75</b> , 1644–1651.

B-dcfn·C <sub>2</sub> H <sub>5</sub> OH	1965857	
B-dcfn·CH <sub>3</sub> OH	1965856	
B-dcfn·2CH <sub>3</sub> OH	1965855	
Clofaziminium (C)		L. Bodart, M. Prinzo, A. Derlet, N. Tumanov and J. Wouters, <i>CrystEngComm</i> , 2021, <b>23</b> , 185-201. <a href="https://doi.org/10.1039/D0CE01400A">https://doi.org/10.1039/D0CE01400A</a>
C·dcfn·MeOH	2032488	
C·dcfn·EtOH	2032489	
C·dcfn·EtOH	2032490	
C·dcfn·CH <sub>3</sub> CN	2032491	
C·dcfn·propiophenone	2032493	
C·dcfn·propiophenone	2032494	
1,3-dihydroxy-2-(hydroxymethyl)propan-2-aminium	1524611	R. Roy, P. Dastidar, <i>Chem. Eur. J.</i> , 2017, <b>23</b> , 15623. <a href="https://doi.org/10.1002/chem.201703850">https://doi.org/10.1002/chem.201703850</a>
Tris(2-Ammonioethyl)amine (taa) 1taa·3dcfn·6H <sub>2</sub> O This is triprotonated tris(2-ethylamine)amine	222868	D. E. Lynch, A. S. Bening and S. Parsons, <i>Acta Crystallogr., Sect. E: Struct. Rep. Online</i> , 2003, <b>59</b> , o1314–o1317, DOI: <a href="https://doi.org/10.1107/S1600536803017926">10.1107/S1600536803017926</a> .
(R)-1-Phenylethylammonium	771712	A. Lemmerer, S. A. Bourne, M. R. Caira, J. Cotton, U. Hendricks, L. C. Peinke and L. Trollope, <i>CrystEngComm</i> , 2010, <b>12</b> , 3634–3641, DOI: <a href="https://doi.org/10.1039/c0ce00043d">10.1039/c0ce00043d</a> .
Pyrrolidinium monohydrate	174825	C. Castellari, F. Comelli and S. Ottani, <i>Acta Crystallogr., Sect. C: Cryst. Struct. Commun.</i> , 2001, <b>57</b> , 1182–1183, DOI: <a href="https://doi.org/10.1107/S0108270101010022">10.1107/S0108270101010022</a> .
Piperizinium dihydrate	129728	C. Castellari and S. Ottani, <i>Acta Crystallogr., Sect. C: Cryst. Struct. Commun.</i> , 1998, <b>54</b> , 415–417, DOI: <a href="https://doi.org/10.1107/S010827019701490X">10.1107/S010827019701490X</a> .
2-aminoethan-1-aminium monohydrate (protonated ethylenediamine)	1480983	P. K. Goswami, V. Kumar, A. Ramanan, <i>J. Mol. Struct.</i> , 2020, <b>1210</b> , 128066. <a href="https://doi.org/10.1016/j.molstruc.2020.128066">https://doi.org/10.1016/j.molstruc.2020.128066</a>
amino{[amino(dimethylamino)methylidene]amino}methaniminium (metformin)	2052795	W.-Q. Feng, L.-Y. Wang, J. Gao, M.-Y. Zhao, Y.-T. Li, Z.-Y. Wu, C.-W. Yan, <i>J. Mol. Struct.</i> , 2021,

		<b>1234,</b> <a href="https://doi.org/10.1016/j.molstruc.2021.130166">https://doi.org/10.1016/j.molstruc.2021.130166</a> 130166.
2-Hydroxyethylammonium monohydrate	2168795	N. Obidova, J. Ashurov, L. Izotova, B. Ibragimov, <i>IUCrData</i> , 2022, <b>7</b> , x220441, DOI: <a href="https://doi.org/10.1107/S2414314622004412">10.1107/S2414314622004412</a>
[Tris-(2-Hydroxymethyl)methyl]ammonium	128603	C. Castellari and S. Ottani, <i>Acta Crystallogr., Sect. C: Cryst. Struct. Commun.</i> , 1997, <b>53</b> , 482–486, DOI: <a href="https://doi.org/10.1107/S0108270196013649">10.1107/S0108270196013649</a> .
Tris(2-Hydroxyethyl)ammonium	127954	C. Castellari and P. Sabatino, <i>Acta Crystallogr., Sect. C: Cryst. Struct. Commun.</i> , 1996, <b>52</b> , 2619–2622, DOI: <a href="https://doi.org/10.1107/S0108270196006300">10.1107/S0108270196006300</a> .
N-(2-Hydroxyethyl)piperidinium	126914	C. Castellari and P. Sabatino, <i>Acta Crystallogr., Sect. C: Cryst. Struct. Commun.</i> , 1996, <b>52</b> , 1708–1712 , DOI: <a href="https://doi.org/10.1107/S0108270196000571">10.1107/S0108270196000571</a> .
N-(2-Hydroxyethyl)morpholinium	126915	C. Castellari and P. Sabatino, <i>Acta Crystallogr., Sect. C: Cryst. Struct. Commun.</i> , 1996, <b>52</b> , 1708–1712, DOI: <a href="https://doi.org/10.1107/S0108270196000571">10.1107/S0108270196000571</a>
N-(2-Hydroxyethyl)piperazinium	126914	C. Castellari and P. Sabatino, <i>Acta Crystallogr., Sect. C: Cryst. Struct. Commun.</i> , 1996, <b>52</b> , 1708–1712, DOI: <a href="https://doi.org/10.1107/S0108270196000571">10.1107/S0108270196000571</a> .
N-(2-Hydroxyethyl)pyrrolidinium	1175199	C. Castellari and P. Sabatino, <i>Acta Crystallogr., Sect. C: Cryst. Struct. Commun.</i> , 1994, <b>50</b> , 1723, DOI: <a href="https://doi.org/10.1107/S0108270194003926">10.1107/S0108270194003926</a> .
Diethanolammonium	126115	C. Castellari, <i>Acta Crystallogr., Sect. C: Cryst. Struct. Commun.</i> , 1995, <b>51</b> , 2612–2615, DOI: <a href="https://doi.org/10.1107/S010827019500730X">10.1107/S010827019500730X</a> .
Diethylammonium monohydrate	163917	C. Castellari, F. Comelli, S. Ottani, <i>Acta Crystallogr., Sect. C: Cryst. Struct. Commun.</i> , 2001, <b>57</b> , 437, DOI: <a href="https://doi.org/10.1107/S010827010002076X">10.1107/S010827010002076X</a> .
Diethylammonium	150469	R. Pomes-Hernandez, J. Duque-Rodriguez, H. Novoa-de-Armas, R.A. Toscano, <i>Zeitschrift fuer Kristallographie - Crystalline Materials</i> , 1997, <b>212</b> , 61, DOI: <a href="https://doi.org/10.1524/zkri.1997.212.1.61">10.1524/zkri.1997.212.1.61</a>  C. Castellari, F. Comelli, S. Ottani, <i>CSD Communication</i> , 2000.

Protonated Norfloxacin	1823915	B. Bhattacharya, A. Mondal, S. R. Soni, S. Das, S. Bhunia, K. B. Raju, A. Ghosh and C. M. Reddy, <i>CrystEngComm</i> , 2018, <b>20</b> , 6420–6429. <a href="https://doi.org/10.1039/C8CE00900G">https://doi.org/10.1039/C8CE00900G</a>
1-Amantadinium	979097	R. Roy, J. Deb, S. S. Jana, P. Dastidar, <i>Chem. Eur. J.</i> , 2014, <b>20</b> , 15320-15324. <a href="https://doi.org/10.1002/chem.201404965">https://doi.org/10.1002/chem.201404965</a>
Choline	N/A	E. Dabrowska-Mas and W. Ras, <i>Curr. Chem. Lett.</i> , 2017, <b>6</b> , 159–166.
2-Amino-2-methyl-1,3-propanediol	N/A	K. M. O'Connor and O. I. Corrigan, <i>Int. J. Pharm.</i> , 2001, <b>226</b> (1–2), 163–179, DOI: <a href="https://doi.org/10.1016/s0378-5173(01)00800-6">10.1016/s0378-5173(01)00800-6</a>
2-Amino-2-methylpropanol	N/A	K. M. O'Connor and O. I. Corrigan, <i>Int. J. Pharm.</i> , 2001, <b>226</b> (1–2), 163–179, DOI: <a href="https://doi.org/10.1016/s0378-5173(01)00800-6">10.1016/s0378-5173(01)00800-6</a> .
<i>tert</i> -Butylammonium	N/A	K. M. O'Connor and O. I. Corrigan, <i>Int. J. Pharm.</i> , 2001, <b>226</b> (1–2), 163–179, DOI: <a href="https://doi.org/10.1016/s0378-5173(01)00800-6">10.1016/s0378-5173(01)00800-6</a> .
Benzylammonium	N/A	K. M. O'Connor and O. I. Corrigan, <i>Int. J. Pharm.</i> , 2001, <b>226</b> (1–2), 163–179, DOI: <a href="https://doi.org/10.1016/s0378-5173(01)00800-6">10.1016/s0378-5173(01)00800-6</a> .
Deanol (2-dimethylaminoethanol)	N/A	K. M. O'Connor and O. I. Corrigan, <i>Int. J. Pharm.</i> , 2001, <b>226</b> (1–2), 163–179, DOI: <a href="https://doi.org/10.1016/s0378-5173(01)00800-6">10.1016/s0378-5173(01)00800-6</a> .

## 2. Fourier Transform Infrared Spectroscopy

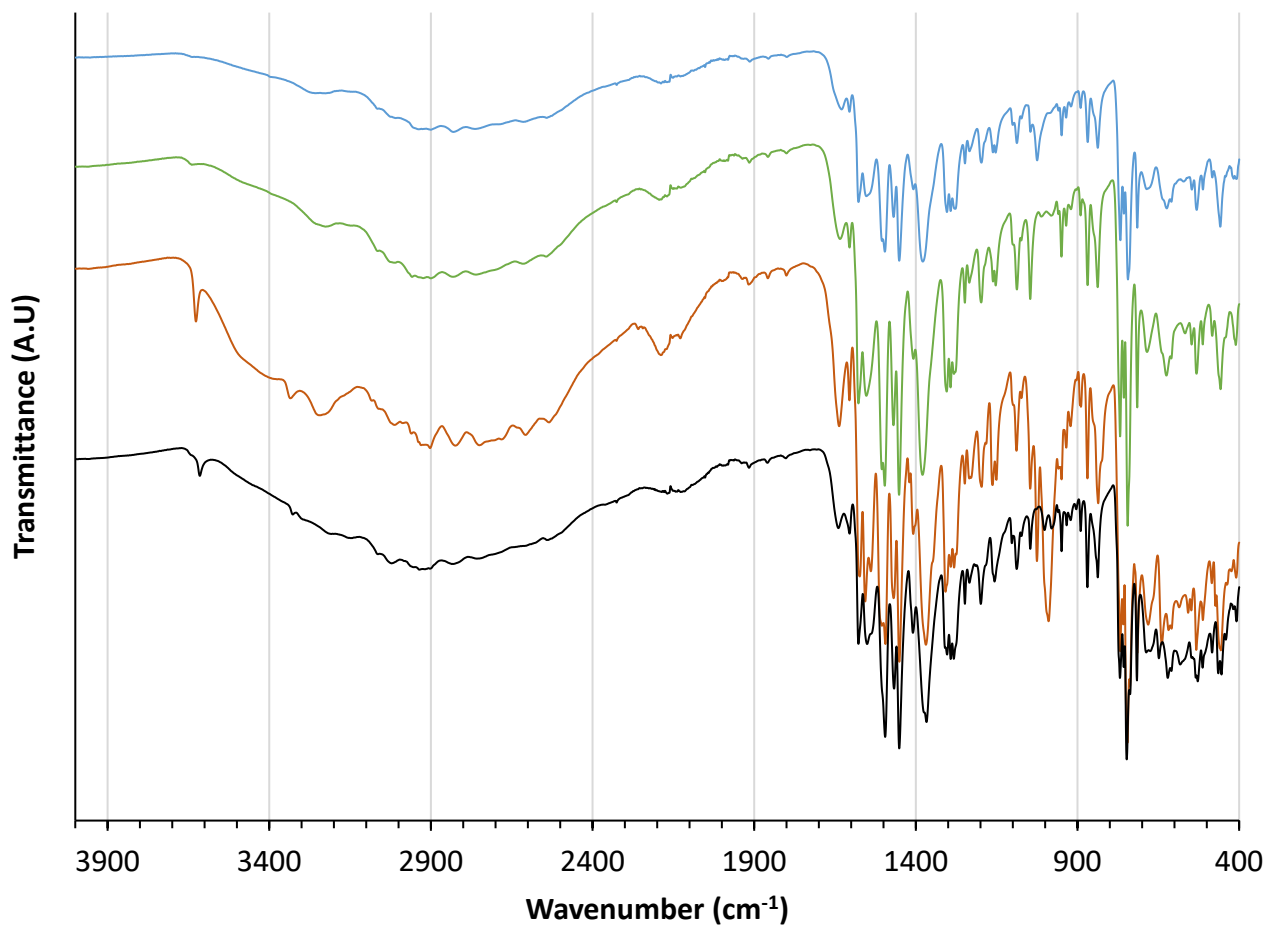


**Figure S 1** FTIR spectra of **1·3H<sub>2</sub>O** (black), **1·2DMSO** (brown), **1·½EtOH·2H<sub>2</sub>O** (green) and **1·2MeOH** (blue). The spectra show a highly conserved nature with the only notable difference observed in **1·2DMSO** being the S-O stretching vibration around 1000 cm<sup>-1</sup>.

### 3. NMR Spectroscopy

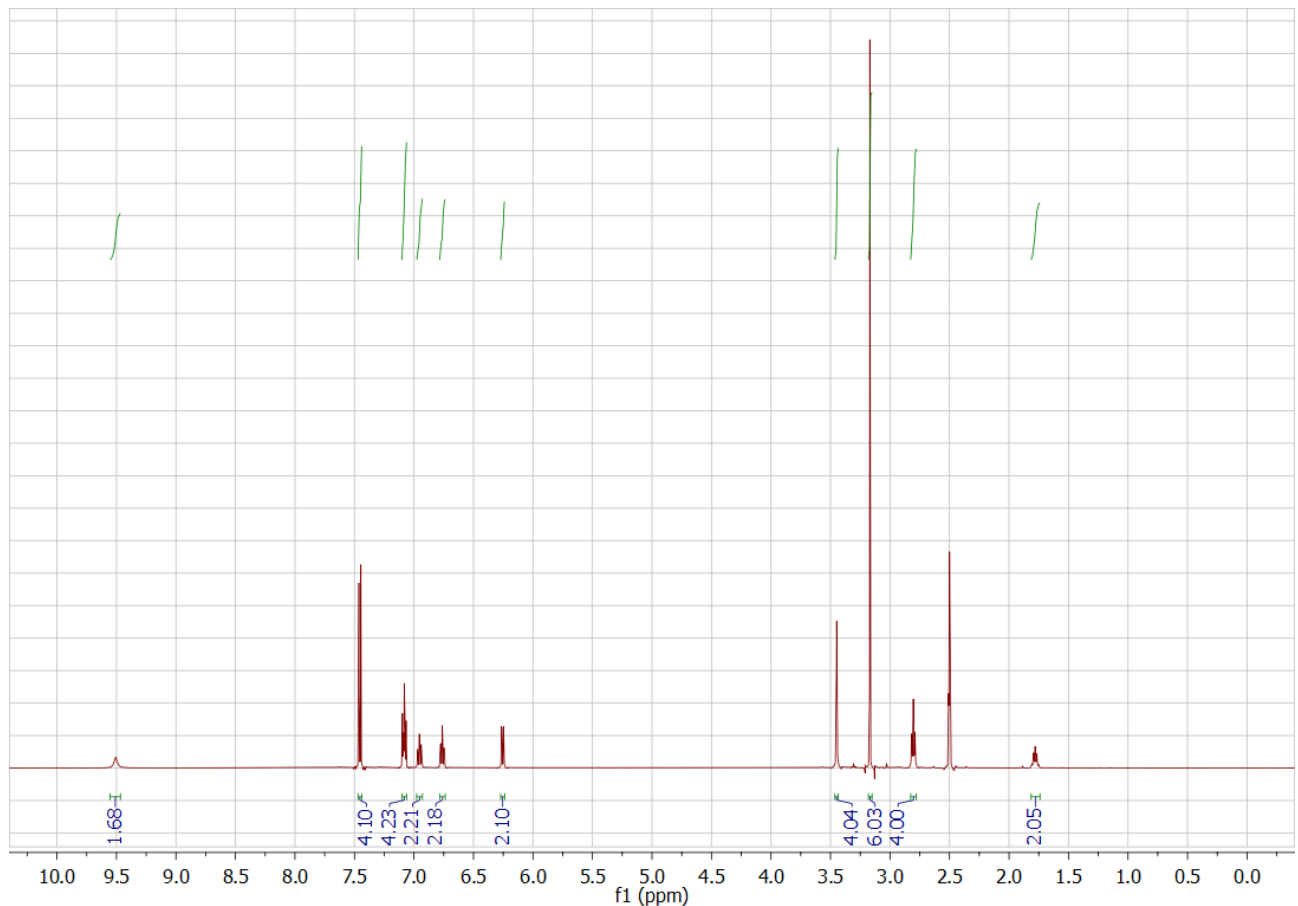


**Figure S 2**  $^1\text{H}$  NMR spectrum in  $\text{DMSO}-d_6$  solution of **1·2MeOH** crystallised from dry MeOH.

Calculation of approximate percentage incorporation of MeOH:

$$\% \text{ Incorporation} = \text{actual incorporation/theoretical incorporation} \times 100/1$$

$$= 6.03/6.00 \times 100/1 = 100\%$$

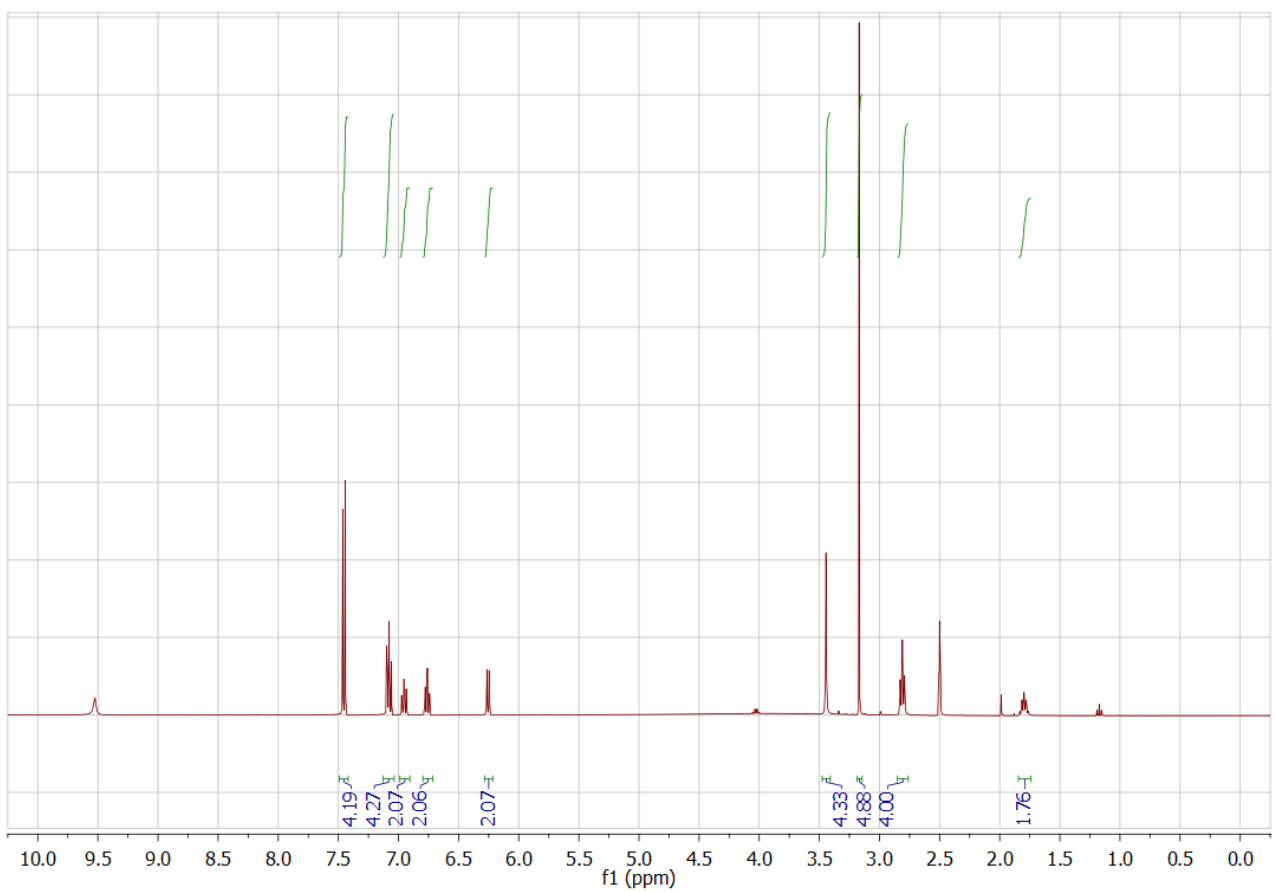


**Figure S 3**  $^1\text{H}$  NMR spectrum in  $\text{DMSO}-d_6$  solution of **1**·2MeOH crystallised from reagent grade MeOH.

Calculation of approximate percentage incorporation of MeOH:

$$\% \text{ Incorporation} = \text{actual incorporation/theoretical incorporation} \times 100/1$$

$$= 4.88/6.00 \times 100/1 = 81\%$$

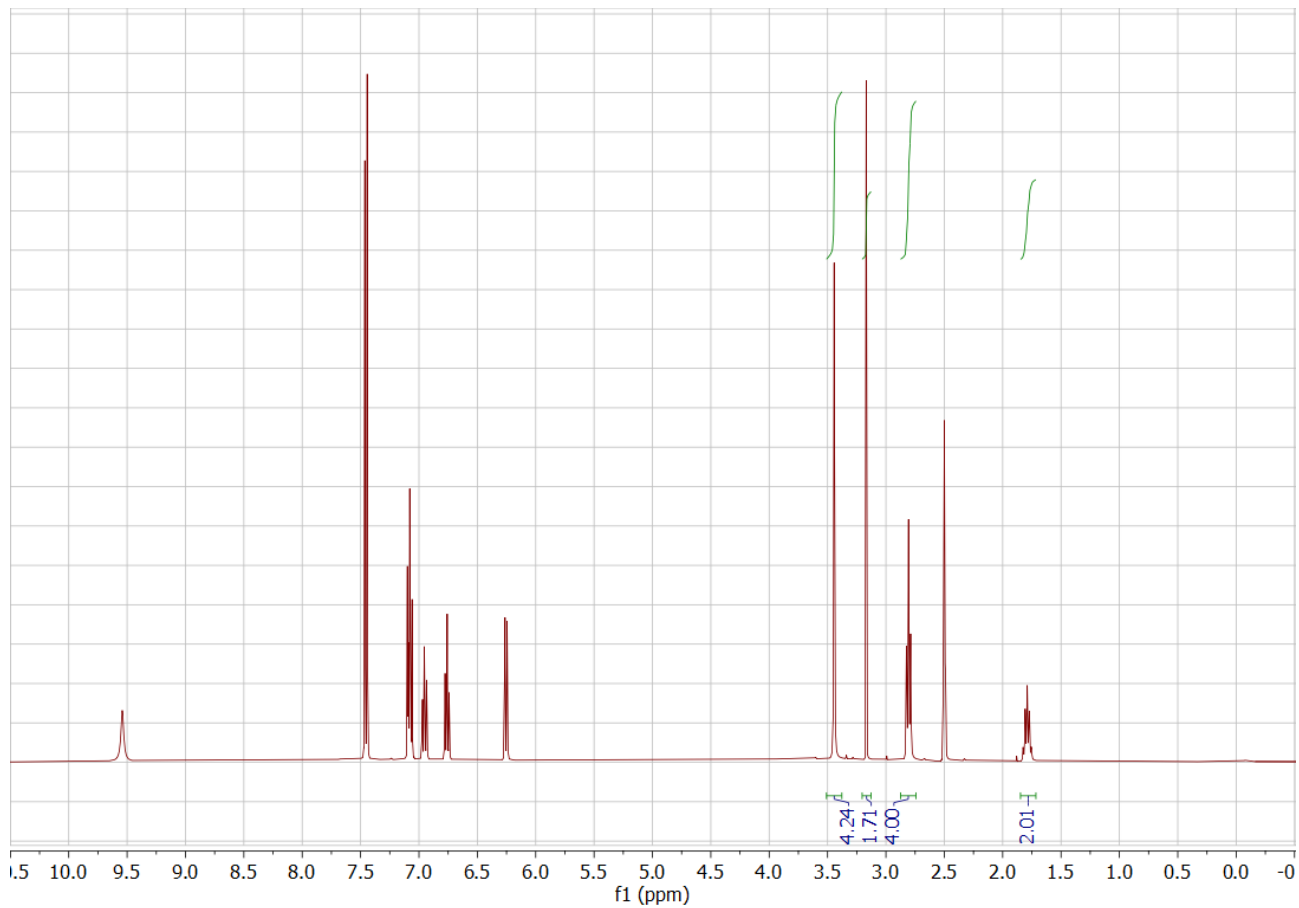


**Figure S 4**  $^1\text{H}$  NMR spectrum in  $\text{DMSO}-d_6$  solution of bulk reaction product crystallised from equal volumes of MeOH and water.

Calculation of approximate percentage incorporation of MeOH:

$$\% \text{ Incorporation} = \text{actual incorporation/theoretical incorporation} \times 100/1$$

$$= 1.71/6.00 \times 100/1 = 28\%$$

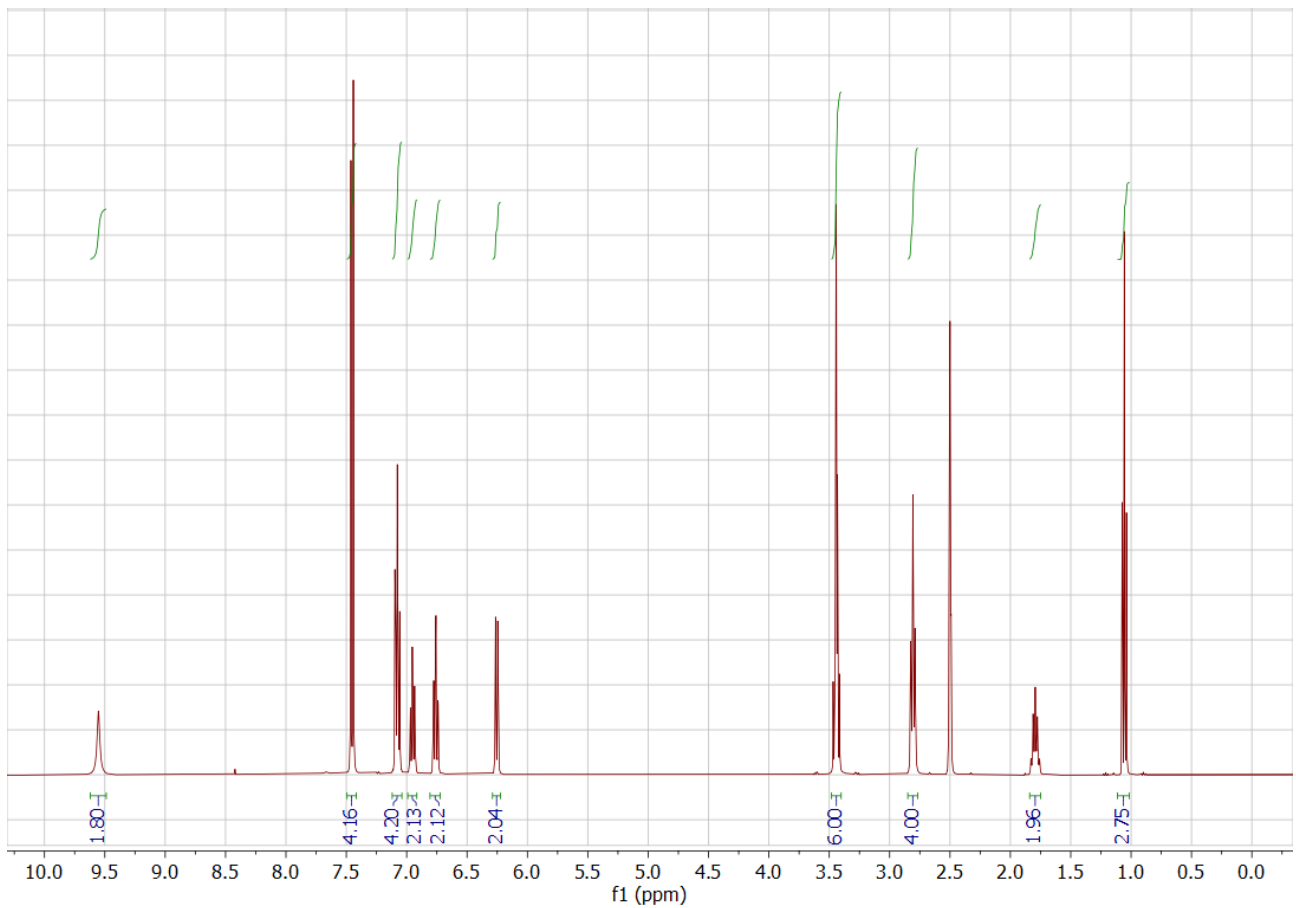


**Figure S 5**  $^1\text{H}$  NMR spectrum in  $\text{DMSO}-d_6$  solution of bulk reaction product crystallised from dry EtOH.

Calculation of approximate percentage incorporation of EtOH:

$$\begin{aligned}\% \text{ Incorporation} &= \text{actual incorporation/theoretical incorporation} \times 100/1 \\ &= 2.75/3.00 \times 100/1 = 92\%\end{aligned}$$

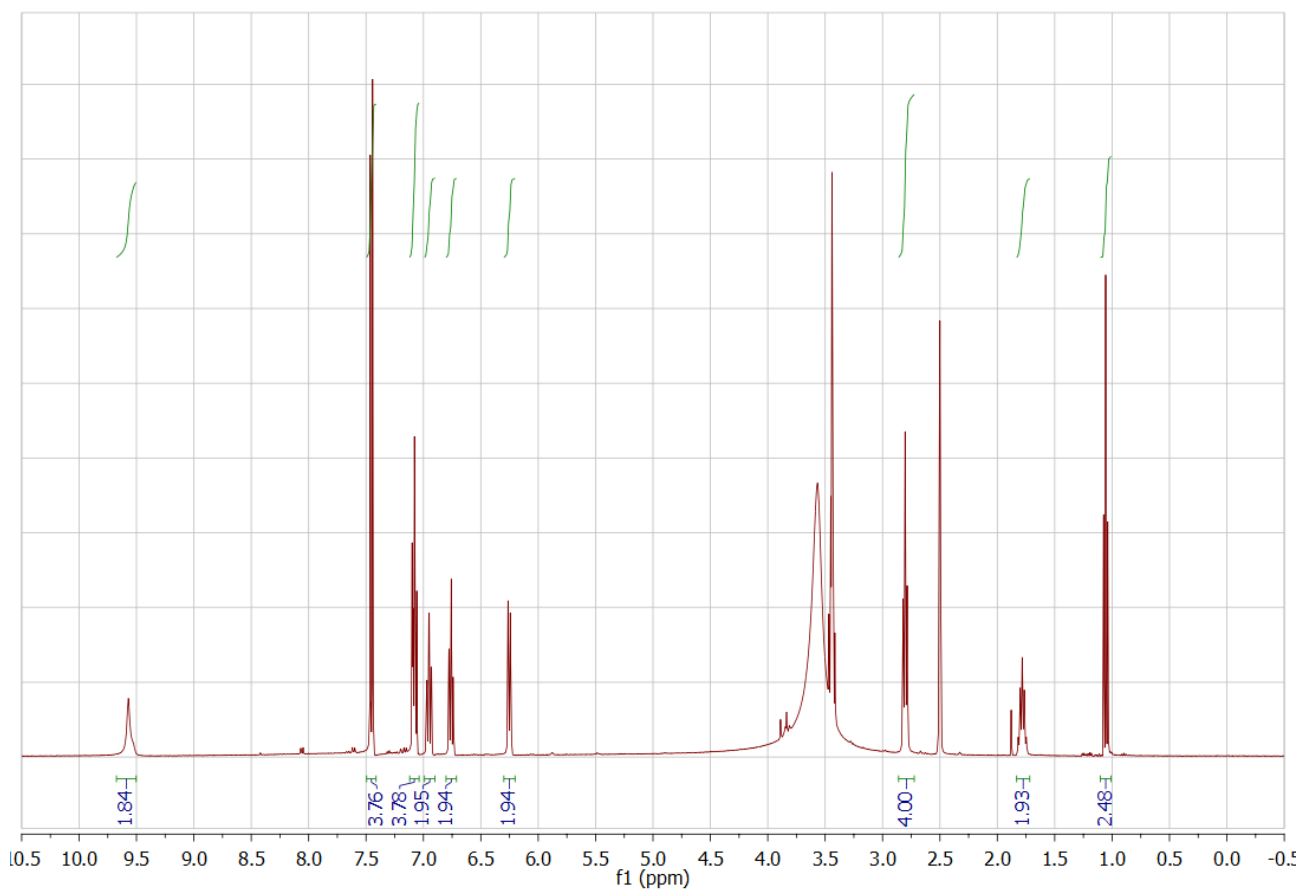


**Figure S 6**  $^1\text{H}$  NMR spectrum in  $\text{DMSO}-d_6$  solution of bulk reaction product crystallised from reagent grade EtOH.

Calculation of approximate percentage incorporation of EtOH:

$$\begin{aligned} \text{\% Incorporation} &= \text{actual incorporation/theoretical incorporation} \times 100/1 \\ &= 2.48/3.00 \times 100/1 = 83\% \end{aligned}$$

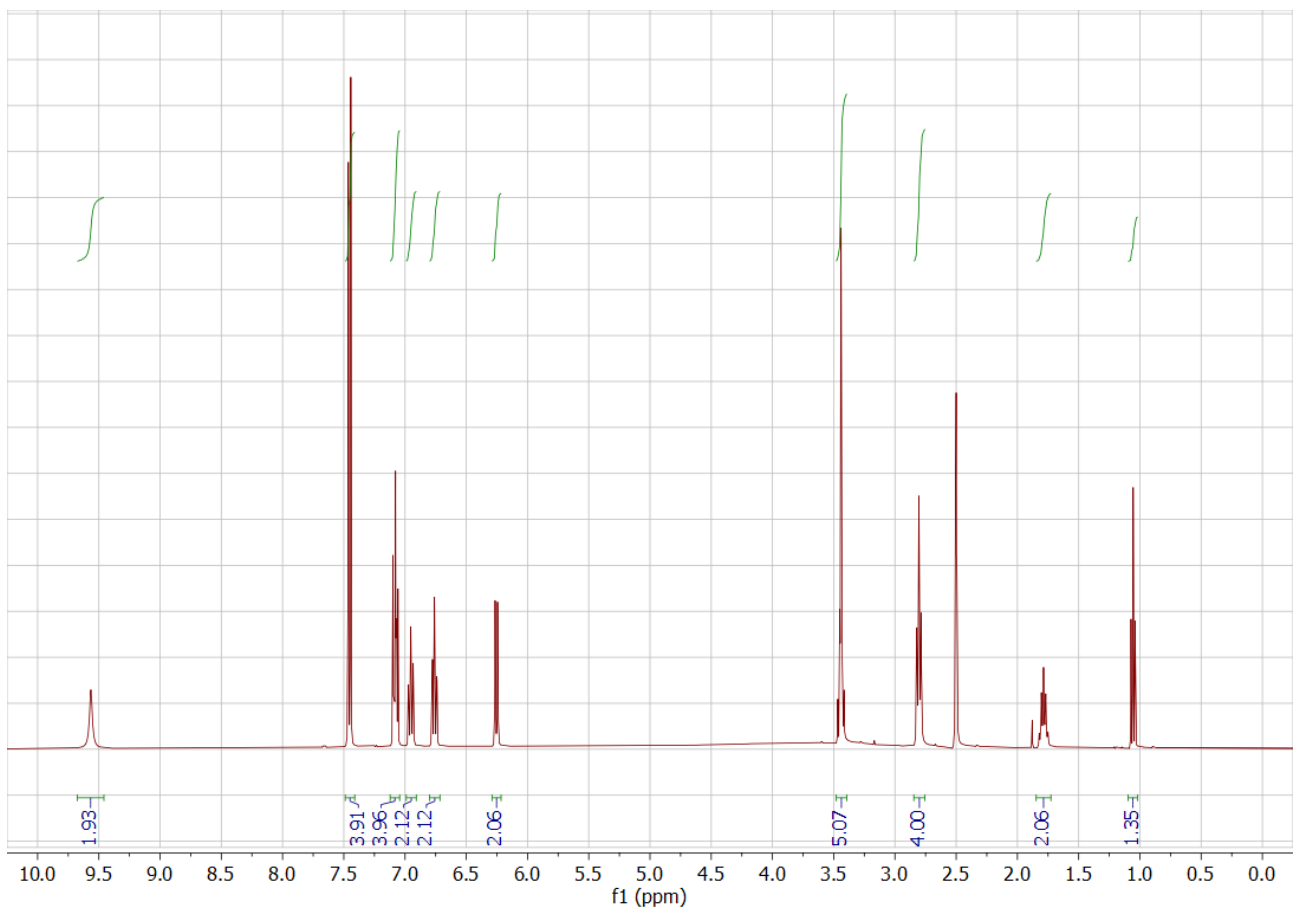


**Figure S 7**  $^1\text{H}$  NMR spectrum in  $\text{DMSO}-d_6$  solution of bulk reaction product crystallised from equal volumes of EtOH and water.

Calculation of approximate percentage incorporation of EtOH:

$$\% \text{ Incorporation} = \text{actual incorporation/theoretical incorporation} \times 100/1$$

$$= 1.35/3.00 \times 100/1 = 45\%$$

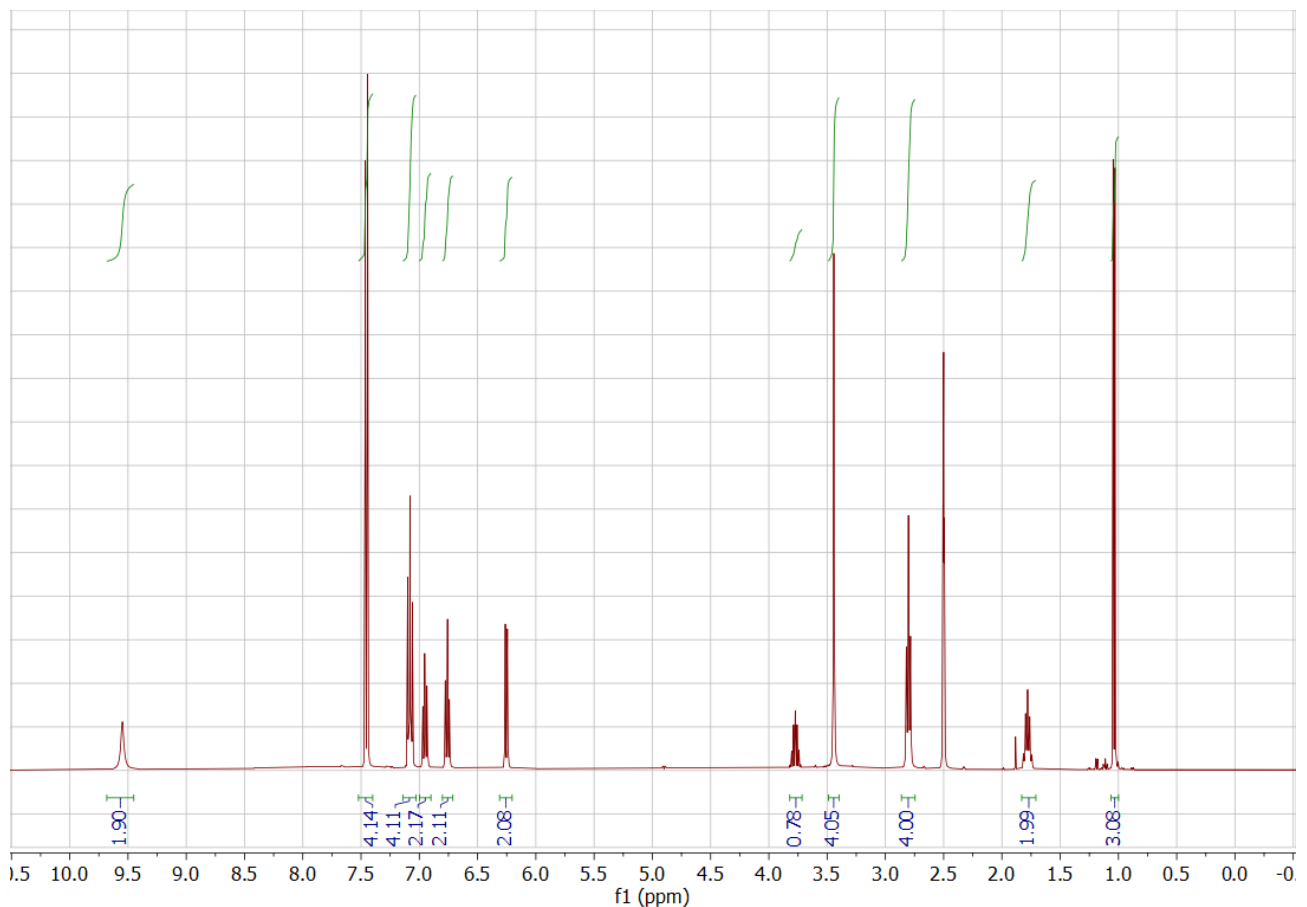


**Figure S 8**  $^1\text{H}$  NMR spectrum in  $\text{DMSO}-d_6$  solution of the bulk crystallised reaction product from  $'\text{PrOH}$ .

Calculation of approximate percentage incorporation of  $'\text{PrOH}$ :

$$\begin{aligned} \text{\% Incorporation} &= \text{actual incorporation/theoretical incorporation} \times 100/1 \\ &= 3.08/6.00 \times 100/1 = 51\% \end{aligned}$$

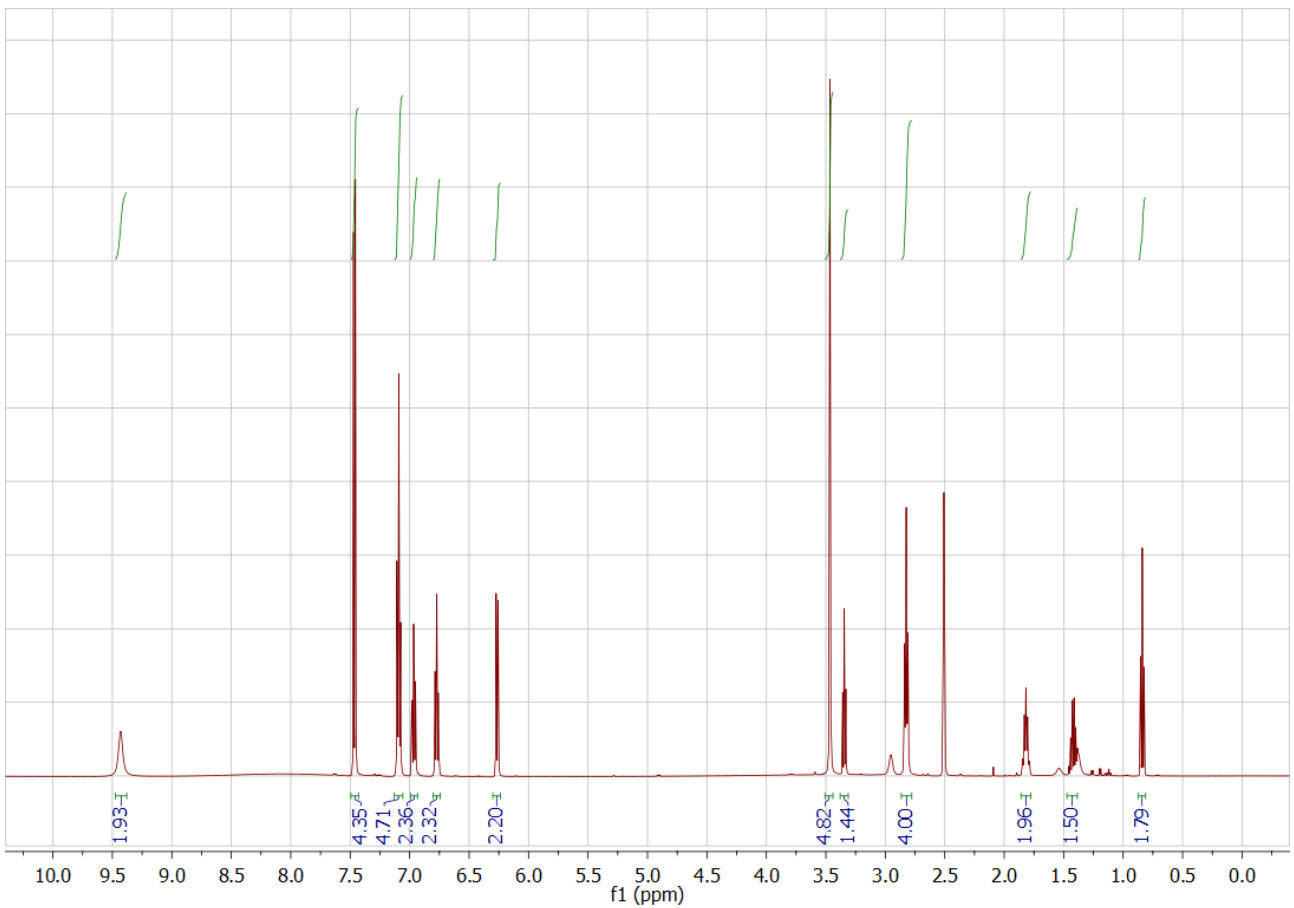


**Figure S 9**  $^1\text{H}$  NMR spectrum in  $\text{DMSO}-d_6$  solution of the bulk crystallised reaction product from  $n\text{PrOH}$ .

Calculation of approximate percentage incorporation of  $n\text{PrOH}$ :

$$\begin{aligned} \text{\% Incorporation} &= \text{actual incorporation/theoretical incorporation} \times 100/1 \\ &= 1.79/3.00 \times 100/1 = 60\% \end{aligned}$$

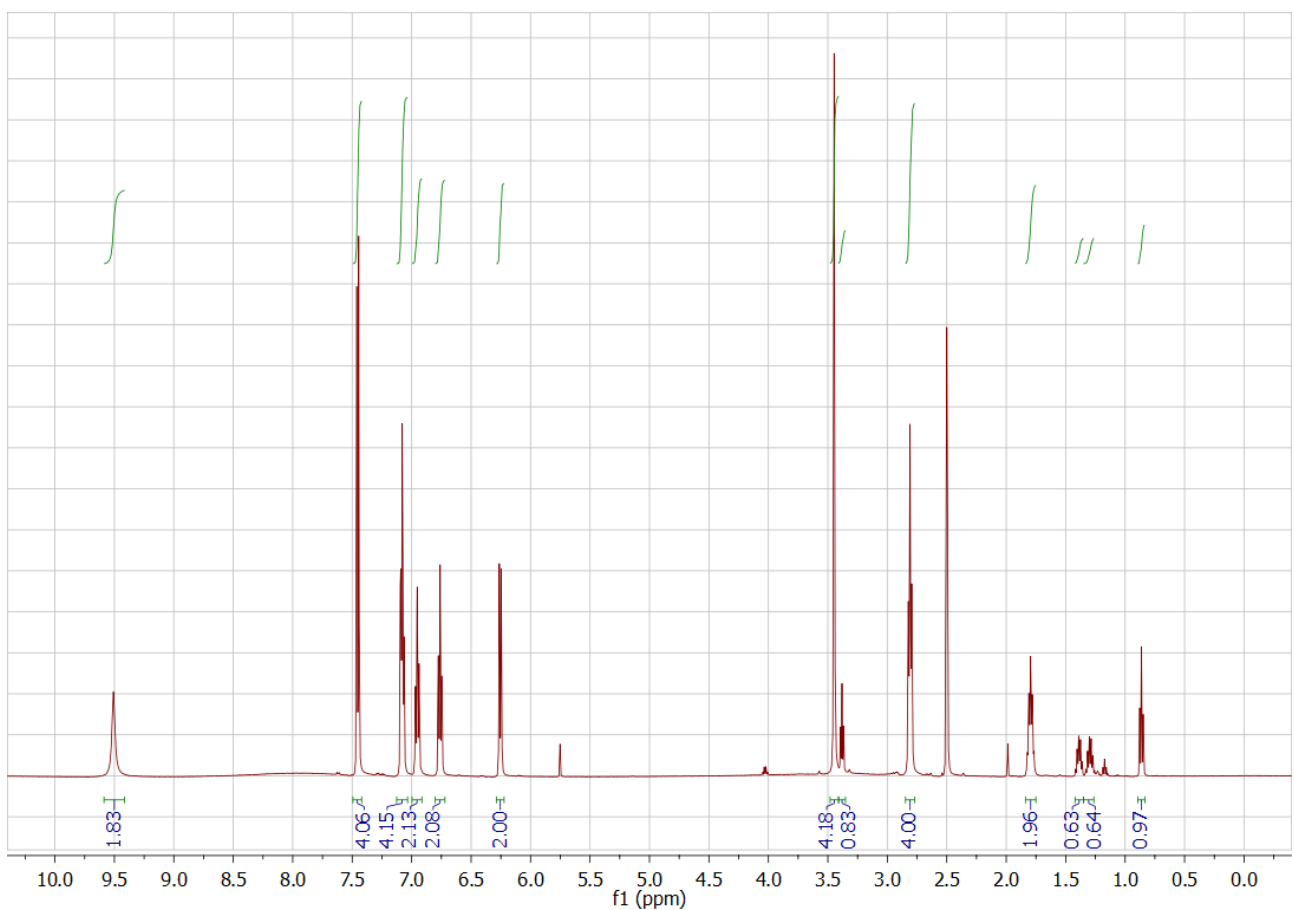


**Figure S 10**  $^1\text{H}$  NMR spectrum in  $\text{DMSO}-d_6$  solution of the bulk crystallised reaction product from  $n\text{BuOH}$ .

Calculation of approximate percentage incorporation of  $n\text{BuOH}$ :

$$\% \text{ Incorporation} = \text{actual incorporation/theoretical incorporation} \times 100/1$$

$$= 0.97/3.00 \times 100/1 = 32\%$$

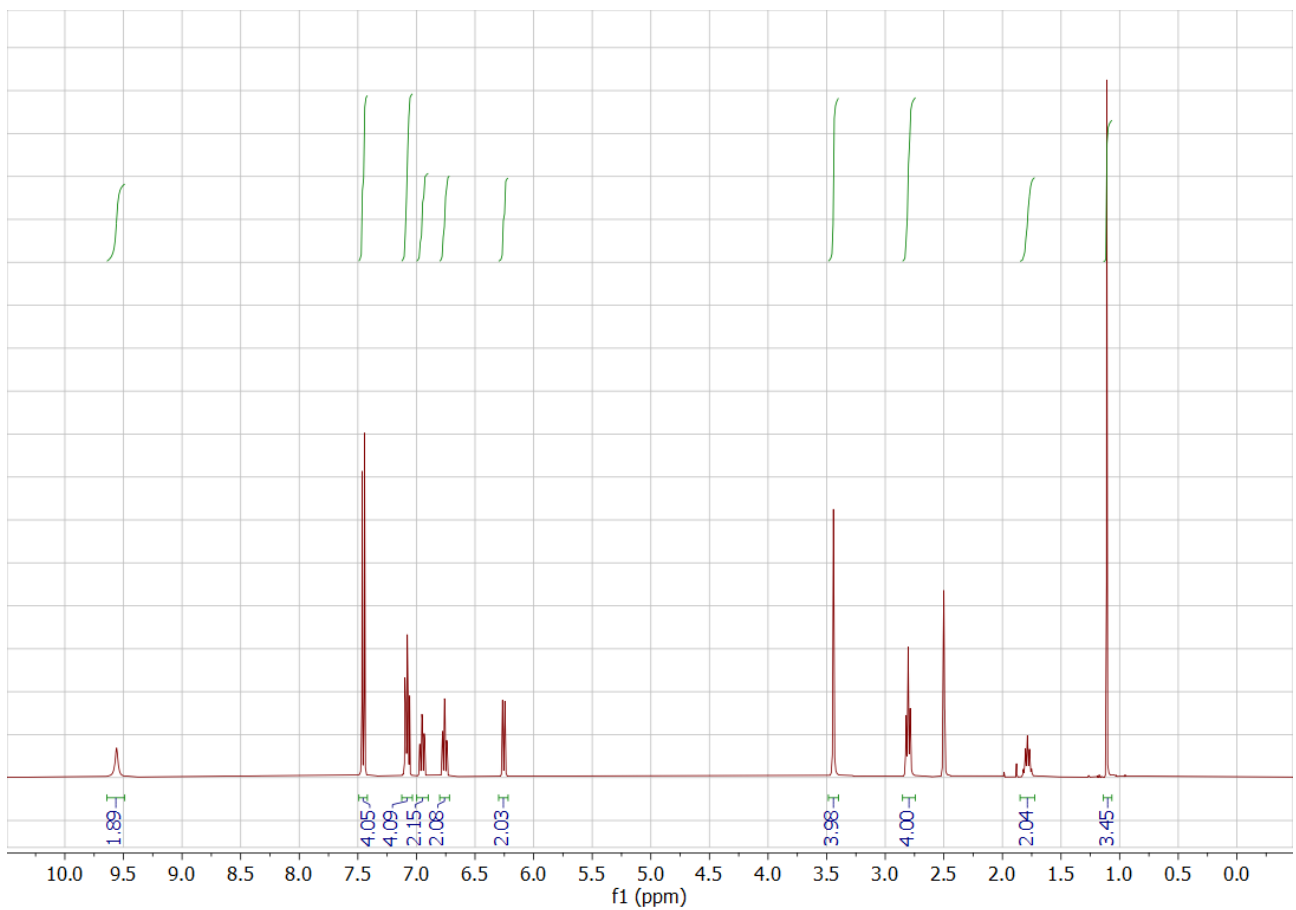


**Figure S 11**  ${}^1\text{H}$  NMR spectrum in  $\text{DMSO}-d_6$  solution of the bulk crystallised reaction product from  ${}^t\text{BuOH}$ .

Calculation of approximate percentage incorporation of  ${}^t\text{BuOH}$ :

$$\begin{aligned}\% \text{ Incorporation} &= \text{actual incorporation/theoretical incorporation} \times 100/1 \\ &= 3.45/9.00 \times 100/1 = 38\%\end{aligned}$$

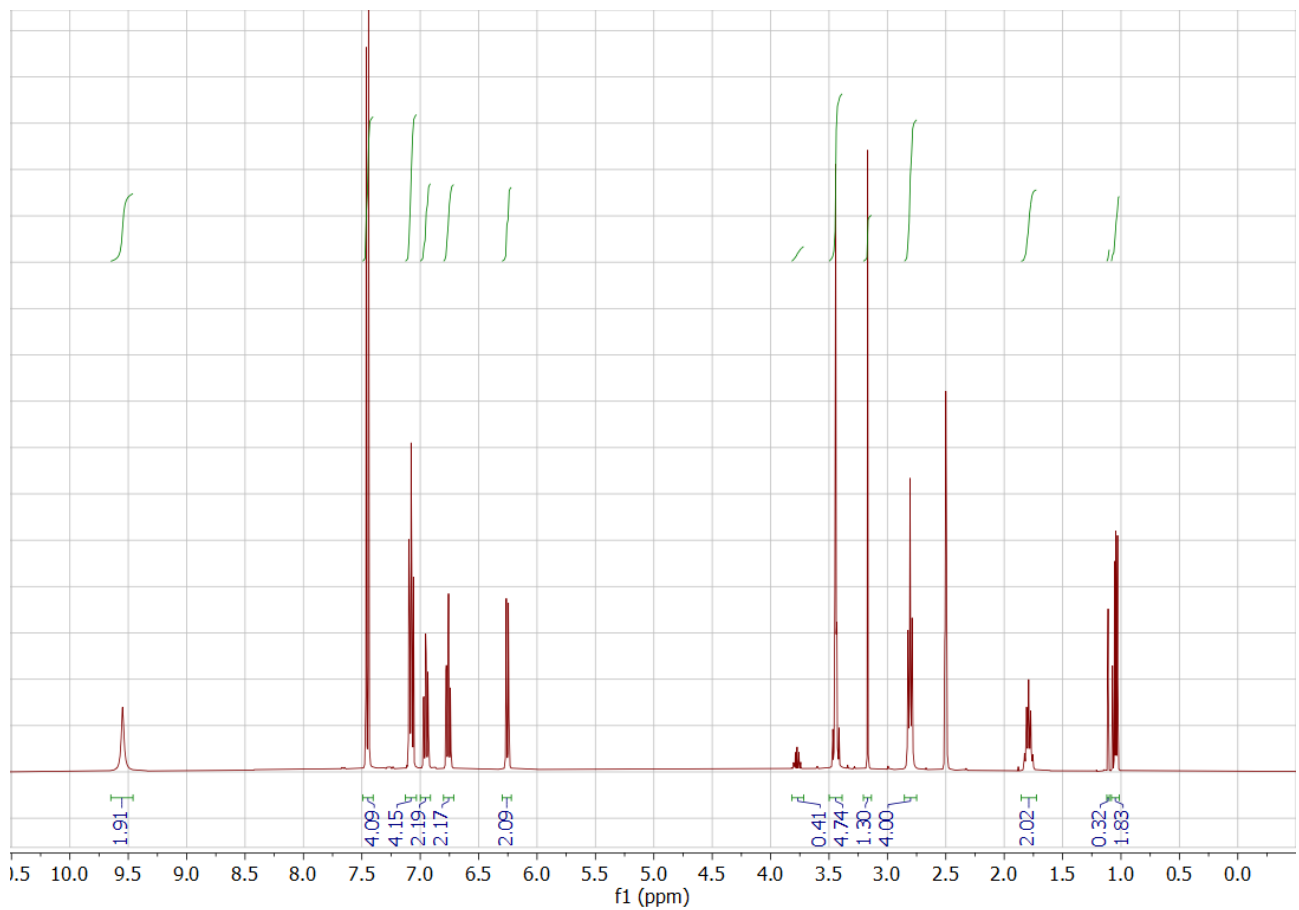


**Figure S 12**  $^1\text{H}$  NMR spectrum in  $\text{DMSO}-d_6$  solution of the bulk crystallised reaction product from an equivolume mixture of dry MeOH, EtOH,  $^1\text{PrOH}$  and  $^t\text{BuOH}$ .

Calculation of approximate ratios for incorporations:

$$\text{dcfn} \quad 2.09/1 = 2.1$$

$$\text{H}_2\text{pn} \quad 4.00/2 = 1$$

$$\text{MeOH} \quad 1.30/3 = 0.43$$

$$\text{EtOH} \quad 0.85/3 = 0.28$$

$$^1\text{PrOH} \quad 0.41/1 = 0.41$$

$$^t\text{BuOH} \quad 0.32/9 = 0.04$$

Formula *sans*  $\text{H}_2\text{O}$ : **1**·0.43MeOH·0.28EtOH·0.41 $^1\text{PrOH}$ ·0.04 $^t\text{BuOH}$

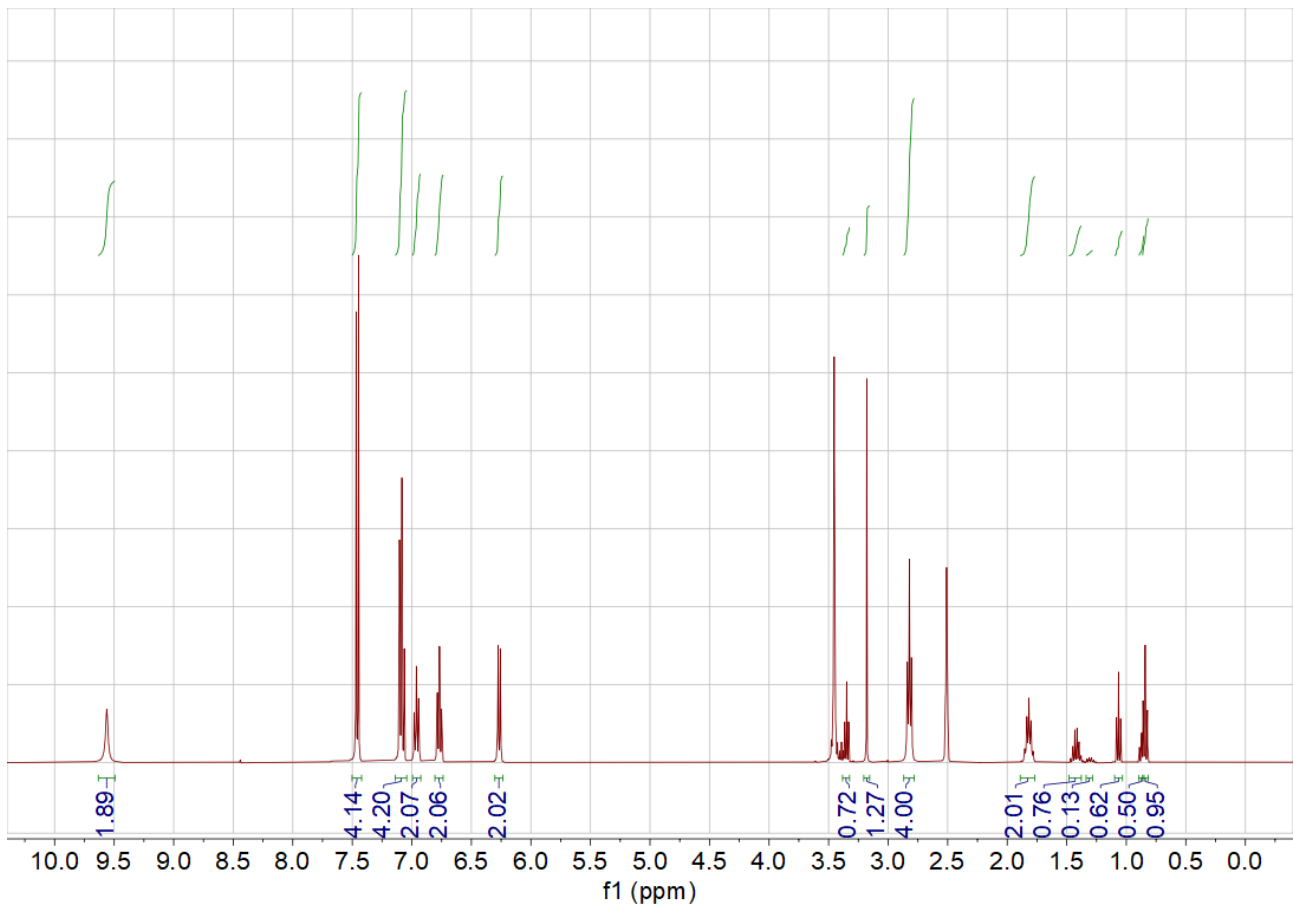


**Figure S 13**  $^1\text{H}$  NMR spectrum in  $\text{DMSO}-d_6$  solution of the bulk crystallised reaction product from an equivolume mixture of dry MeOH, EtOH,  $^n\text{PrOH}$  and  $^n\text{BuOH}$ .

Calculation of approximate ratios for incorporations:

$$\text{dcfn} \quad 2.02/1 = 2.0$$

$$\text{H}_2\text{pn} \quad 4.00/4 = 1$$

$$\text{MeOH} \quad 1.27/3 = 0.42$$

$$\text{EtOH} \quad 0.62/3 = 0.21$$

$$^n\text{PrOH} \quad 0.81/3 = 0.27$$

$$^n\text{BuOH} \quad 0.27/3 = 0.09$$

Formula *sans*  $\text{H}_2\text{O}$ : **1**·0.42MeOH·0.21EtOH·0.27 $^n\text{PrOH}$ ·0.09 $^n\text{BuOH}$

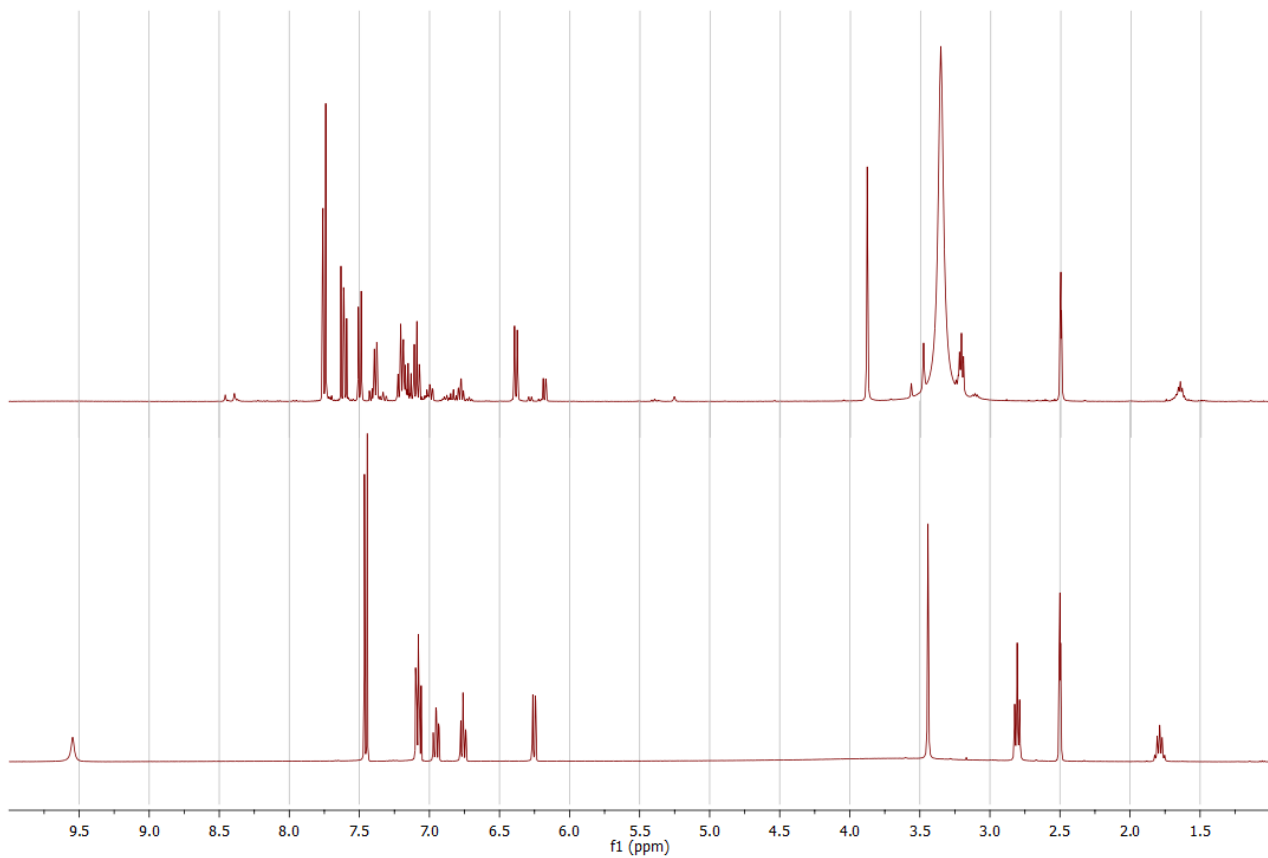


**Figure S 14** <sup>1</sup>H NMR spectra in DMSO-*d*<sub>6</sub> solutions of **1·3H<sub>2</sub>O** (bottom) and the crude product obtained by heating to 200 °C (top).

## 4. Single Crystal X-ray Diffraction

**Table S 2**

Identification code	1·3H <sub>2</sub> O (exp_269)	1·2DMSO (exp_375)	1·2MeOH (exp_351)
Empirical formula	C <sub>31</sub> H <sub>38</sub> N <sub>4</sub> O <sub>7</sub> Cl <sub>4</sub>	C <sub>17.5</sub> H <sub>22</sub> Cl <sub>2</sub> N <sub>2</sub> O <sub>3</sub> S	C <sub>33</sub> H <sub>40</sub> Cl <sub>4</sub> N <sub>4</sub> O <sub>6</sub>
Formula weight	720.45	411.33	730.49
Temperature/K	150(1)	294(1)	294(1)
Crystal system	Triclinic	Orthorhombic	Triclinic
Space group	P-1	Pccn	P-1
a/Å	9.4328(2)	9.6066(5)	9.6753(3)
b/Å	9.8482(3)	43.035(2)	9.9173(3)
c/Å	18.3159(7)	9.7812(5)	19.0010(5)
$\alpha/^\circ$	90.907(3)	90	88.365(2)
$\beta/^\circ$	94.232(2)	90	79.728(3)
$\gamma/^\circ$	90.018(2)	90	88.551(3)
Volume/Å <sup>3</sup>	1696.62(9)	4043.7(4)	1792.87(10)
Z	2	8	2
$\rho_{\text{calc}} \text{g/cm}^3$	1.410	1.351	1.353
$\mu/\text{mm}^{-1}$	0.401	0.443	0.378
F(000)	752.0	1720.0	764.0
Crystal size/mm <sup>3</sup>	0.32 × 0.24 × 0.11	0.51 × 0.19 × 0.05	0.6 × 0.6 × 0.35
Radiation	MoK $\alpha$ ( $\lambda = 0.71073$ )	Mo K $\alpha$ ( $\lambda = 0.71073$ )	Mo K $\alpha$ ( $\lambda = 0.71073$ )
2 $\Theta$ range for data collection/°	4.136 to 61.316	5.104 to 60.774	4.11 to 56.564
Index ranges	-12 ≤ h ≤ 13, -13 ≤ k ≤ 13, -13 ≤ l ≤ 13, -60 ≤ l ≤ 59, -25 ≤ l ≤ 25	-12 ≤ h ≤ 12, -13 ≤ k ≤ 13, -25 ≤ l ≤ 25	-12 ≤ h ≤ 12, -13 ≤ k ≤ 13, -25 ≤ l ≤ 25
Reflections collected	32176	43370	34574
Independent reflections	9830 [R <sub>int</sub> = 0.0338, R <sub>sigma</sub> = 0.0543]	5935 [R <sub>int</sub> = 0.0430, R <sub>sigma</sub> = 0.0407]	8719 [R <sub>int</sub> = 0.0250, R <sub>sigma</sub> = 0.0235]
Data/restraints/parameters	9830/9/461	5935/79/273	8719/50/482
Goodness-of-fit on F <sup>2</sup>	1.041	1.040	1.035
Final R indexes [I>=2σ(I)]	R <sub>1</sub> = 0.0437, wR <sub>2</sub> = 0.0981	R <sub>1</sub> = 0.0664, wR <sub>2</sub> = 0.1703	R <sub>1</sub> = 0.0438, wR <sub>2</sub> = 0.1159
Final R indexes [all data]	R <sub>1</sub> = 0.0807, wR <sub>2</sub> = 0.1116	R <sub>1</sub> = 0.1095, wR <sub>2</sub> = 0.1903	R <sub>1</sub> = 0.0629, wR <sub>2</sub> = 0.1265
Largest diff. peak/hole / e Å <sup>-3</sup>	0.36/-0.30	0.89/-0.36	0.29/-0.33
CCDC	2076682	2210150	2210151

Identification code	<b>1</b> ·EtOH·2H <sub>2</sub> O (exp_392)	<b>1</b> ·H <sub>2</sub> O (exp_396)	<b>1</b> ·iPrOH (Twincr_twin2_hklf4)
Empirical formula	C <sub>33.01</sub> H <sub>42.01</sub> Cl <sub>4</sub> N <sub>4</sub> O <sub>7</sub>	C <sub>31</sub> H <sub>40</sub> Cl <sub>4</sub> N <sub>4</sub> O <sub>8</sub>	C <sub>34</sub> H <sub>40</sub> Cl <sub>4</sub> N <sub>4</sub> O <sub>5</sub>
Formula weight	748.57	738.47	726.50
Temperature/K	294(1)	295(1)	100(1) K
Crystal system	Triclinic	monoclinic	Triclinic
Space group	P-1	P2 <sub>1</sub>	P-1
a/Å	9.4529(4)	9.35740(10)	9.4880(3)
b/Å	10.1381(2)	36.5523(5)	9.7666(3)
c/Å	19.0267(6)	10.2282(2)	18.9486(7)
$\alpha^{\circ}$	84.791(2)	90	88.206(3)
$\beta^{\circ}$	89.345(3)	90.1340(10)	78.488(3)
$\gamma^{\circ}$	88.234(2)	90	88.798(3)
Volume/Å <sup>3</sup>	1814.95(10)	3498.39(9)	1719.52(10)
Z	2	4	2
$\rho_{\text{calc}}/\text{cm}^3$	1.370	1.402	1.403
$\mu/\text{mm}^{-1}$	0.377	0.392	3.519
F(000)	784.0	1544.0	760.0
Crystal size/mm <sup>3</sup>	0.41 × 0.21 × 0.12	0.53 × 0.41 × 0.21	0.36 × 0.09 × 0.04
Radiation	Mo K $\alpha$ ( $\lambda = 0.71073$ )	Mo K $\alpha$ ( $\lambda = 0.71073$ )	Cu K $\alpha$ ( $\lambda = 1.54184$ )
2 $\Theta$ range for data collection/ $^{\circ}$	4.036 to 59.146	3.982 to 60.782	9.06 to 157.05
Index ranges	-13 ≤ h ≤ 13, -14 ≤ k ≤ 14, -25 ≤ l ≤ 26	-13 ≤ h ≤ 13, -51 ≤ k ≤ 51, -14 ≤ l ≤ 14	-11 ≤ h ≤ 12, -9 ≤ k ≤ 12, -21 ≤ l ≤ 23
Reflections collected	59277	155834	17521
Independent reflections	9918 [R <sub>int</sub> = 0.0348, R <sub>sigma</sub> = 0.0368]	20631 [R <sub>int</sub> = 0.0286, R <sub>sigma</sub> = 0.0238]	6716 [R <sub>int</sub> = 0.0826, R <sub>sigma</sub> = 0.0557]
Data/restraints/parameters	9918/83/537	20631/7/901	6716/1/434
Goodness-of-fit on F <sup>2</sup>	1.035	1.029	1.083
Final R indexes [I>=2σ(I)]	R <sub>1</sub> = 0.0612, wR <sub>2</sub> = 0.1748	R <sub>1</sub> = 0.0333, wR <sub>2</sub> = 0.0743	R <sub>1</sub> = 0.0770, wR <sub>2</sub> = 0.2267
Final R indexes [all data]	R <sub>1</sub> = 0.0997, wR <sub>2</sub> = 0.2047	R <sub>1</sub> = 0.0471, wR <sub>2</sub> = 0.0795	R <sub>1</sub> = 0.0916, wR <sub>2</sub> = 0.2583
Largest diff. peak/hole / e Å <sup>-3</sup>	0.75/-0.89	0.20/-0.29	0.72/-0.80
Flack parameter		-0.028(7)	
CCDC	2246041	2245278	2245277

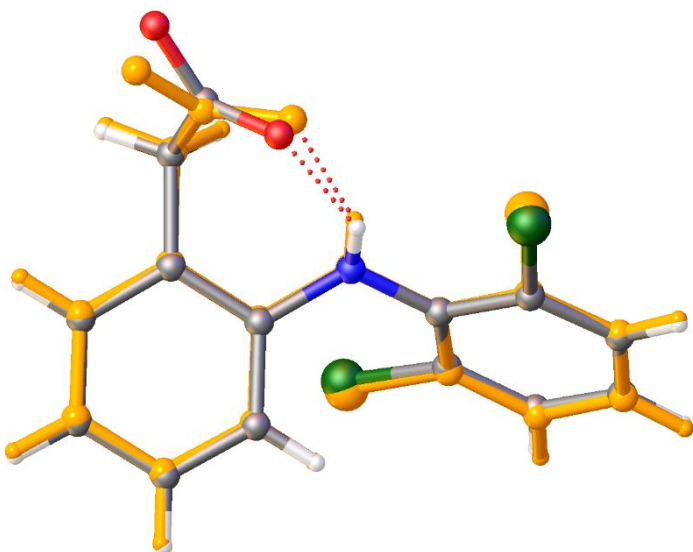


**Figure S 15** Overlay of the two dcfn anions in the asymmetric unit of **1**·3H<sub>2</sub>O. One molecule is coloured orange for clarity.

**Table S 3** Table of H-Bond donor-acceptor (D-A) distances from propane-1,3-diaminium cations in **1**·3H<sub>2</sub>O.

D	H	A	D-H (Å)	H-A (Å)	D-A (Å)	D-H-A (°)
N1S	H1SA	O3W#	0.91	1.89	2.785(2)	166.6
N1S	H1SB	O2A#	0.91	1.92	2.818(2)	168.3
N1S	H1SC	O1A#	0.91	2.47	3.158(2)	132.9
N1S	H1SC	O2A^	0.91	2.01	2.903(2)	168.6
C2S	H2SA	O2B	0.99	2.35	3.295(2)	159.4
C3S	H3SB	O1A#	0.99	2.51	3.277(2)	133.9
N5S	H5SA	O1W'	0.91	1.93	2.814(2)	163.8
N5S	H5SB	O2W''	0.91	2.44	3.040(2)	123.8
N5S	H5SB	O2W	0.91	2.05	2.864(2)	148.7
N5S	H5SC	O2B	0.91	1.86	2.759(2)	168.5

Symmetry codes: ' = 1-X,1-Y,1-Z; '' = 1-X,2-Y,1-Z; ^ = +X,1+Y,+Z; # = 2-X,1-Y,1-Z.

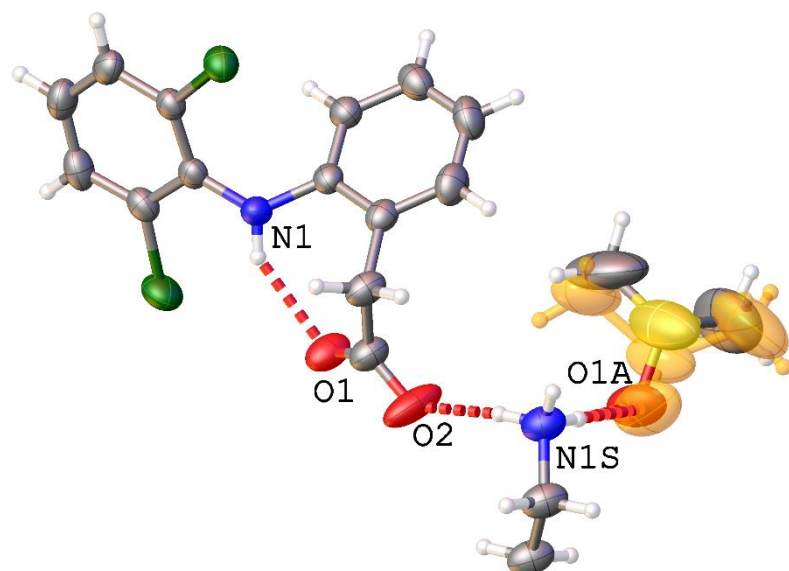


**Figure S 16** Asymmetric unit of **1·2DMSO** with selected atomic labelling. ADPs are displayed at the 50% probability level. The minor component (0.48) of the disordered DMSO molecule is shaded in orange.  
 $O1 \cdots H1 2.14(2)$  Å,  $O2 \cdots H1SB 1.85(3)$  Å,  $O1A \cdots H1SC 2.02(2)$  Å.

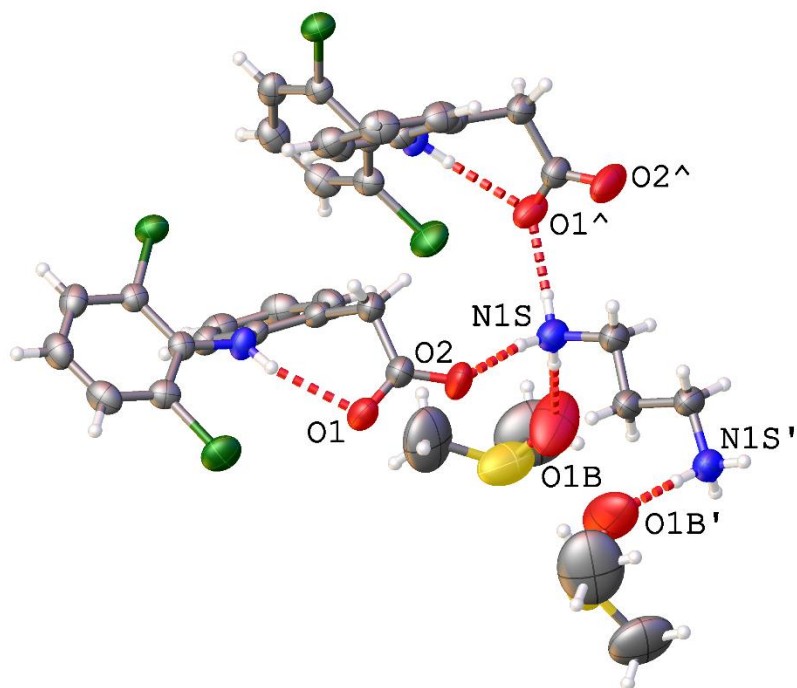


**Figure S 17** A perspective view of the formula unit in **1·2DMSO** with selected atom labelling. Hydrogen bonding interactions are displayed as red dashed lines. Only one position of the disordered DMSO molecules is shown. ADPs are displayed at the 50% probability level. Symmetry codes: ' =  $3/2-X, 3/2-Y, +Z$ ; ^ =  $3/2-X, +Y, -1/2+Z$ .

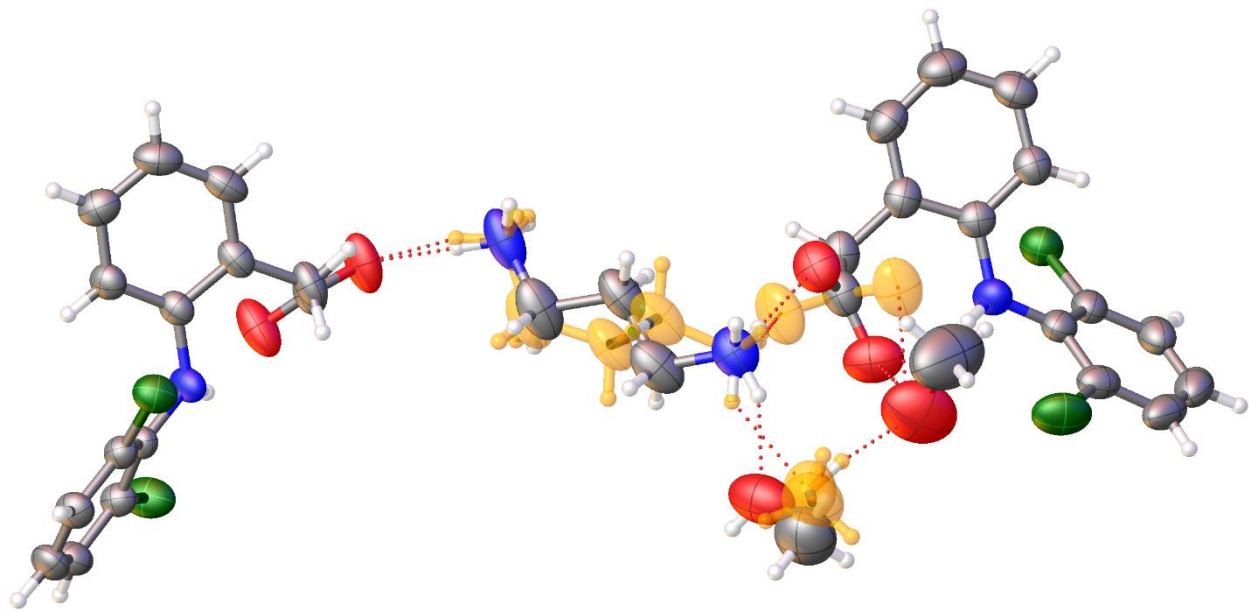


**Figure S 18** A perspective view of the asymmetric unit of **1**·2MeOH. Hydrogen bonding interactions are displayed as red dotted lines. The minor occupancy position of the disorder in the carboxylate group (0.39), propane-1,3-diaminium cation (0.11) and methanol molecule (0.33) are shaded in orange. ADPs are displayed at the 50% probability level.

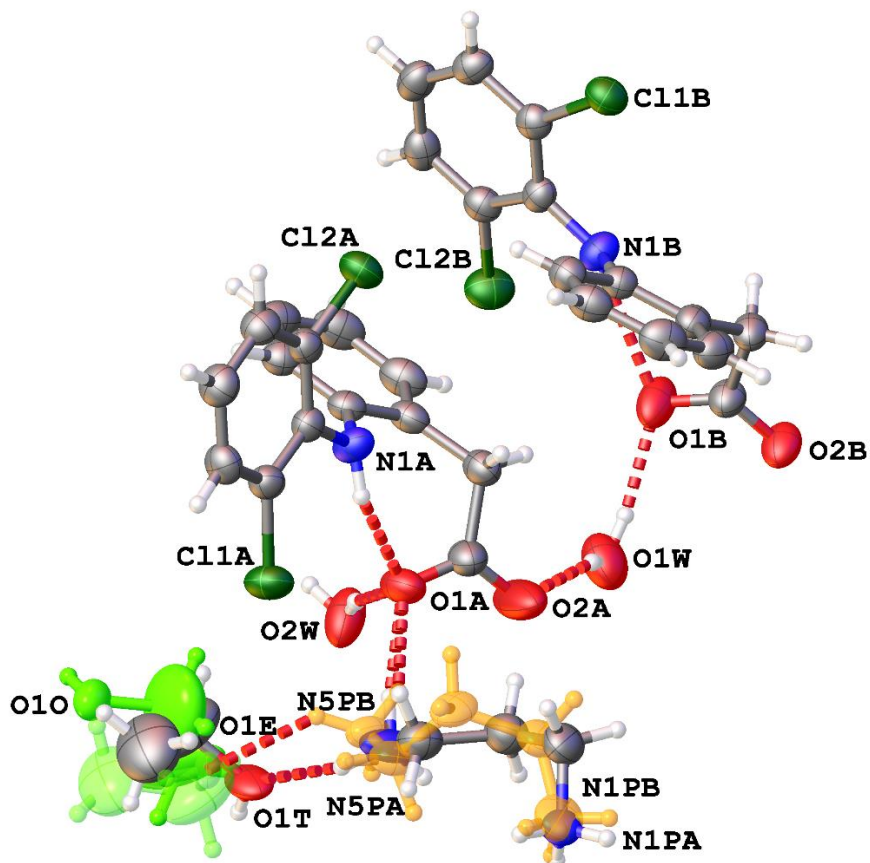


**Figure S 19** A perspective view of the asymmetric unit of **1**·EtOH·2H<sub>2</sub>O with selected atomic labelling. Hydrogen bonding interactions are displayed as red dashed lines. The minor occupancy position of the disorder in the propane-1,3-diaminium cation (0.43) is shaded in orange. The minor occupancy positions of the ethanol molecules are displayed in green. ADPs are displayed at the 50% probability level.

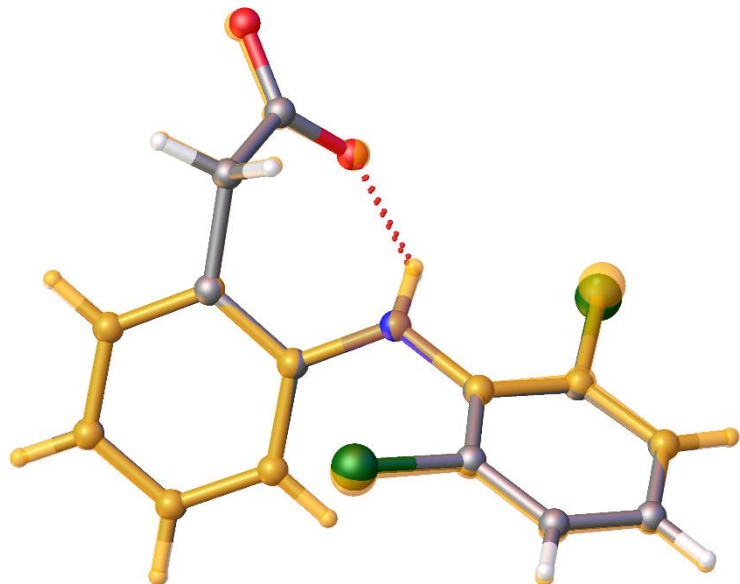


**Figure S 20** Overlay of the two dcfn anions in the asymmetric unit of **1·EtOH·2H<sub>2</sub>O**. One molecule is coloured orange for clarity.

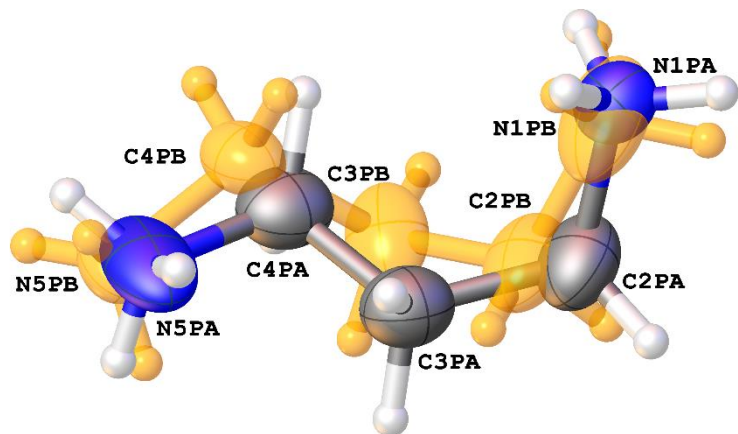


**Figure S 21** View of the disordered propane-1,3-diaminium cation in the asymmetric unit of **1·EtOH·2H<sub>2</sub>O**. The minor occupancy *gauche-gauche* conformer (0.43) is coloured orange. ADPs are displayed at the 50% probability level.

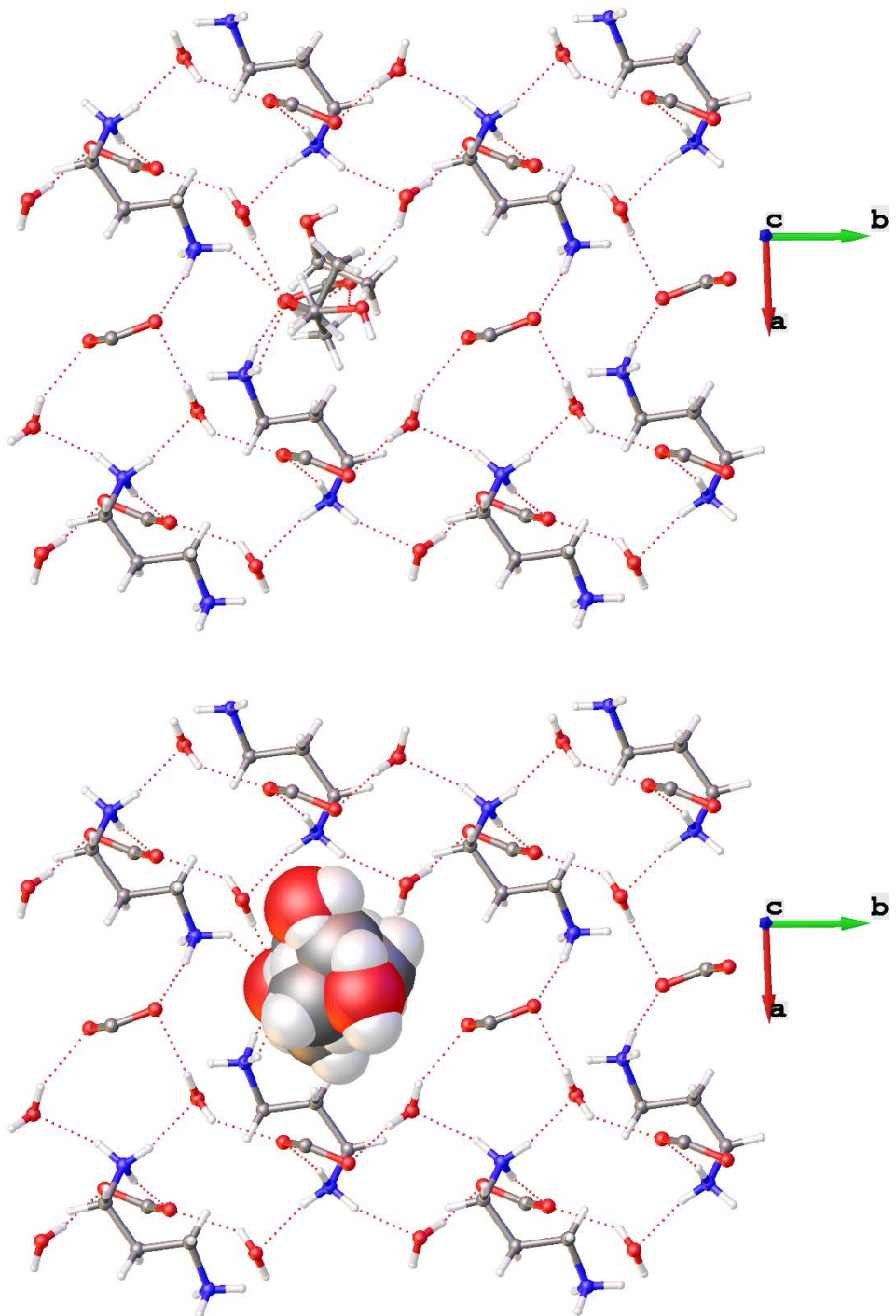


**Figure S 22** Views of the pocket that the disordered ethanol molecule occupies in the structure of **1·EtOH·2H<sub>2</sub>O**. The representation at the top shows the disorder and the representation at the bottom shows the ethanol in space filling form to accentuate the pocket. Only the major conformer of the H<sub>2</sub>pn cations is shown, for clarity.

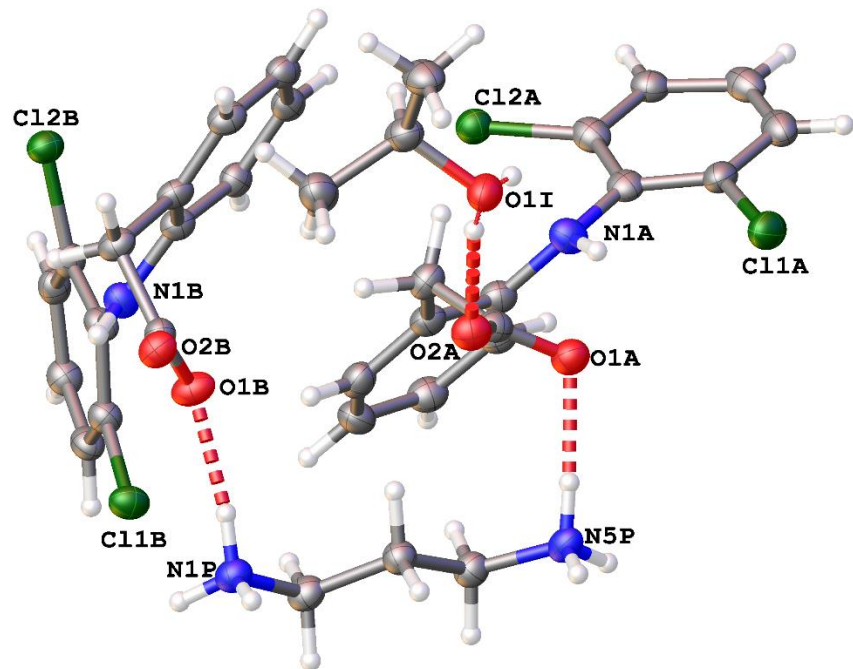


**Figure S 23** A perspective view of the asymmetric unit of **1**-*i*PrOH with selected atomic labelling. Both positions of the hydrogen attached to O1I (0.78:0.22) are shown. Hydrogen bonding interactions are displayed as red dashed lines. H5PB···O1A 1.818(3) Å; H1PC···O1B 1.898(3) Å; O2A···H1I 1.876(3) Å. ADPs are displayed at the 50% probability level.

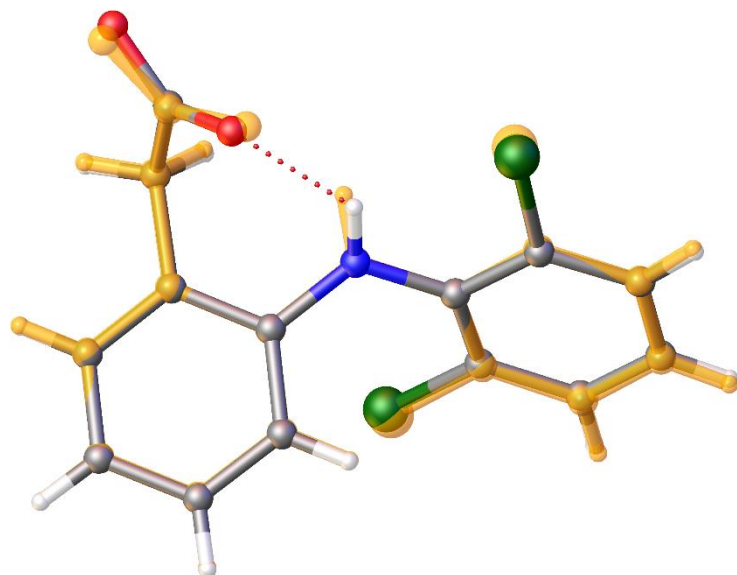


**Figure S 24** Overlay of the two dcfn anions in the asymmetric unit of **1**-*i*PrOH. One molecule is coloured orange for clarity.

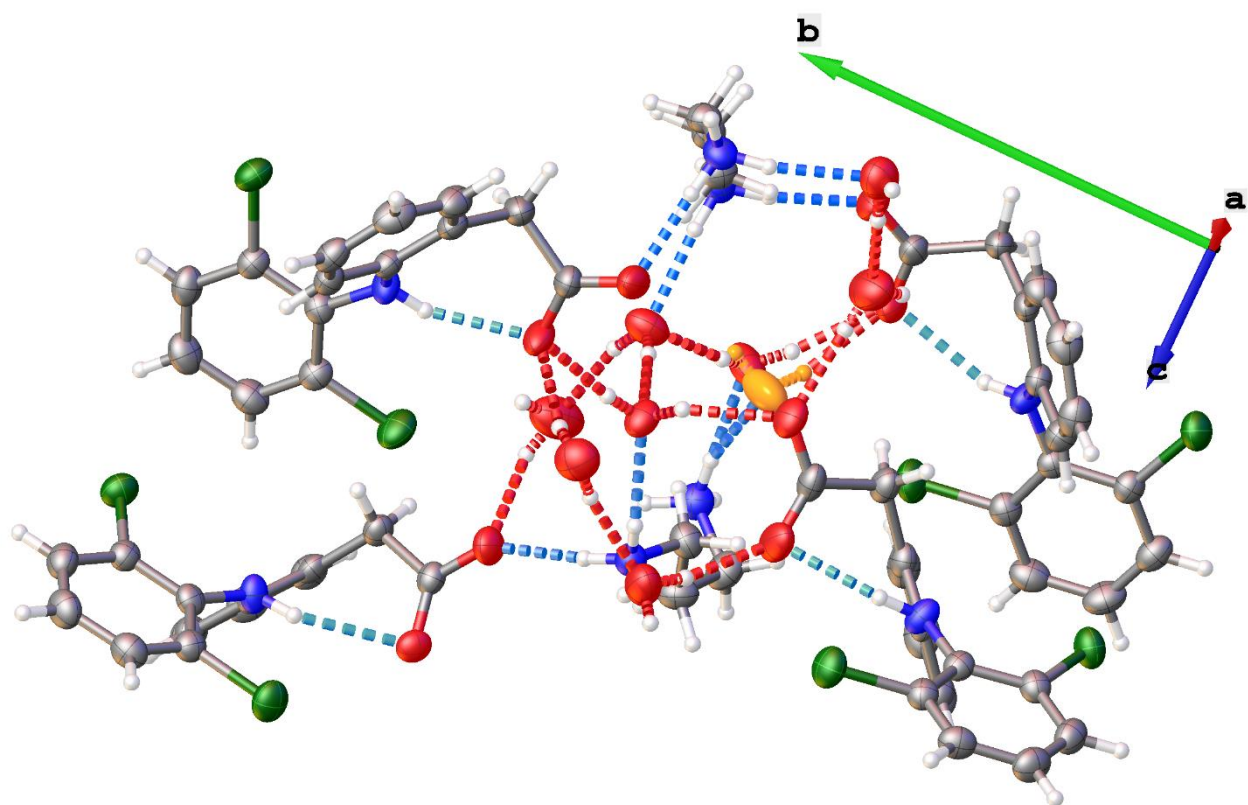


**Figure S 25** A perspective view of the asymmetric unit of **1**·2H<sub>2</sub>O. Hydrogen bonding interactions are displayed as dashed lines based on the parent hydrogen donor atom (red for oxygen and blue for nitrogen; the intramolecular dcfn hydrogen bonds are light blue and those from H<sub>2</sub>pn cations are dark blue). The minor contributor to the disordered water position (0.23) is coloured orange. ADPs are displayed at the 50% probability level.

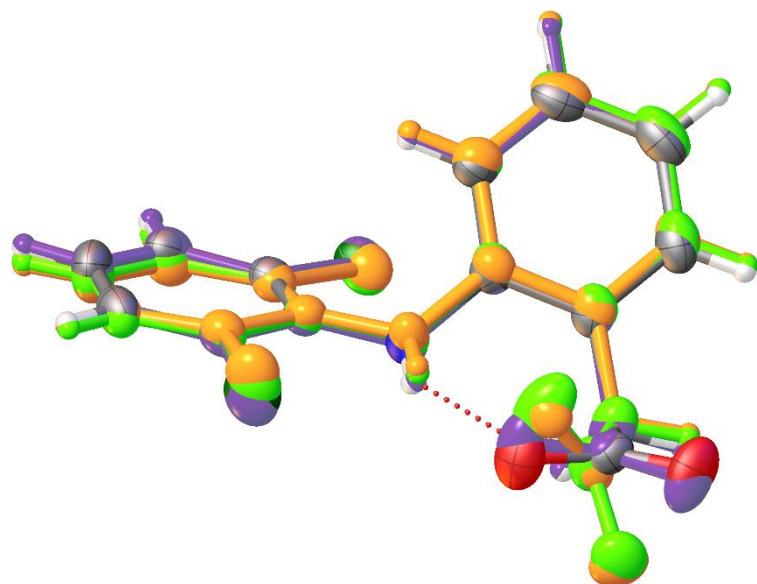


**Figure S 26** Overlay of the dcfn anions in the asymmetric unit of **1**·2H<sub>2</sub>O. One pair of molecules are coloured orange and green and the other red and purple. The main difference is the orientations of the carboxyl group.

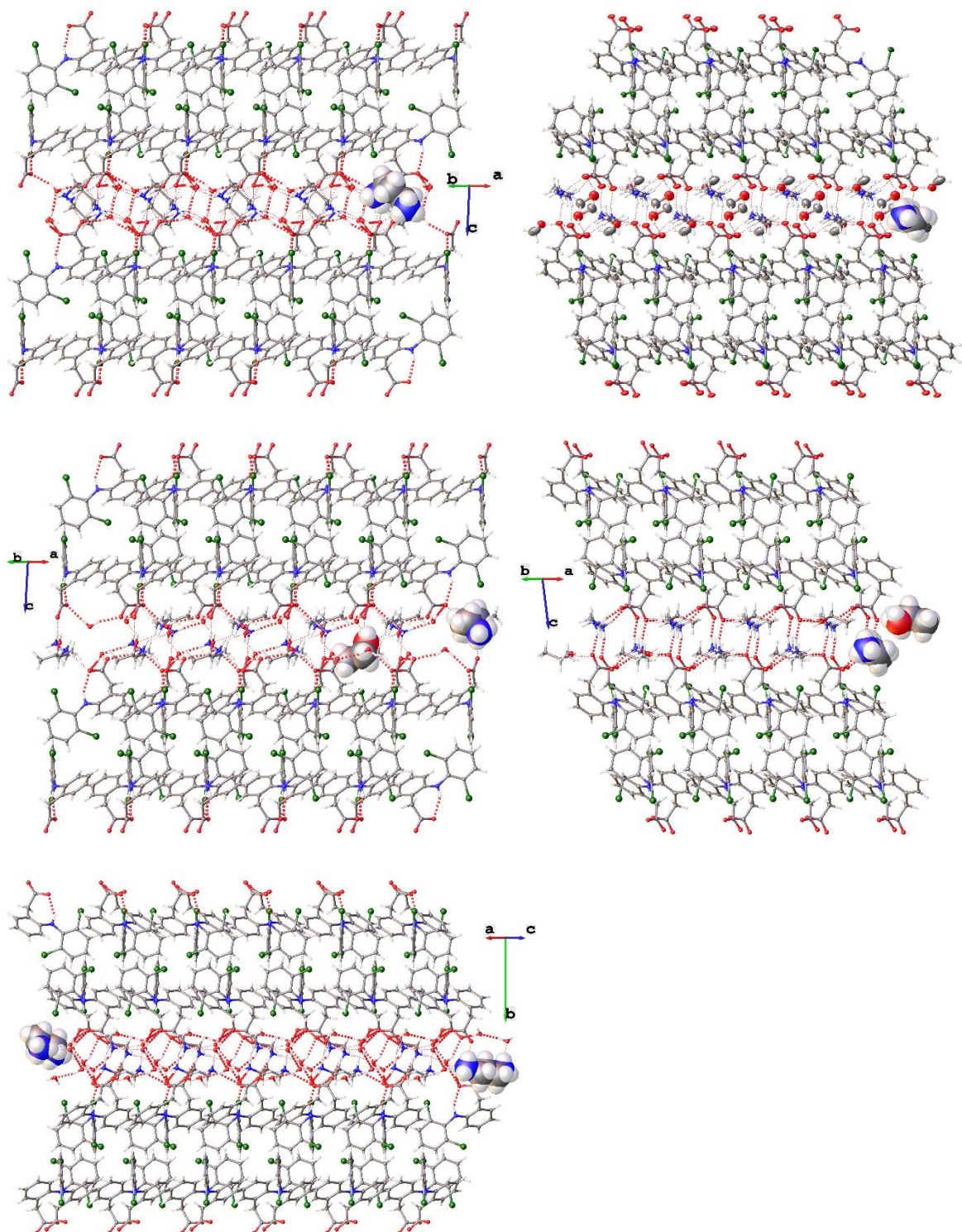


**Figure S 27** Views along the 110 directions showing the structural similarity in **1·3H<sub>2</sub>O** (top left), **1·2MeOH** (top right), **1·EtOH·2H<sub>2</sub>O** (middle left), **1·PrOH** (middle right). The view for **1·2H<sub>2</sub>O** (bottom left) is shown in the 101 direction. One molecule of propane-1,3-diaminium is shown in space filling representation in the hydrophilic layer of **1·3H<sub>2</sub>O**, **1·2MeOH**, **1·EtOH·2H<sub>2</sub>O**, and **1·PrOH** as a guide to its orientation. Two molecules are shown in the view of **1·2H<sub>2</sub>O** because it has two unique H<sub>2</sub>pn cations in the ASU.

## 5. Powder X-Ray Diffraction

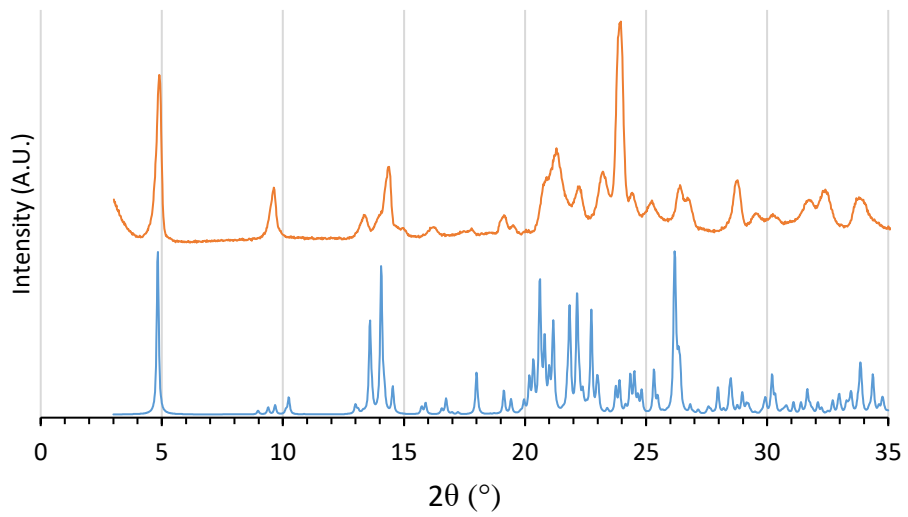


**Figure S 28** Calculated (blue) and experimental (orange) patterns of **1·3H<sub>2</sub>O** synthesised in solution.

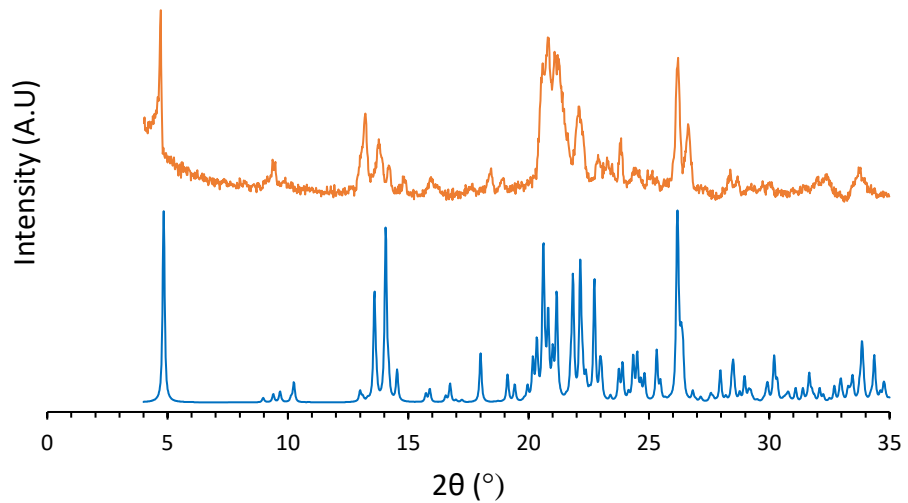


**Figure S 29** Calculated (blue) and experimental pattern (orange) of mechanochemically-synthesised **1·3H<sub>2</sub>O**.

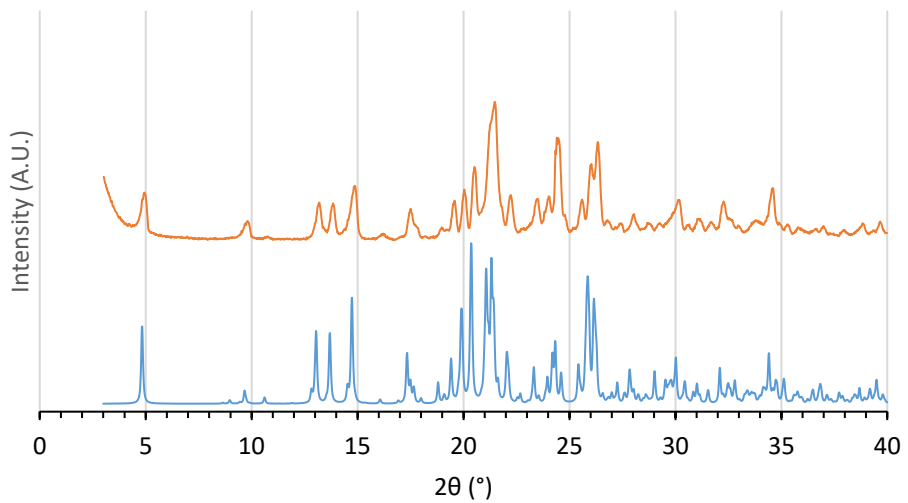


**Figure S 30** Calculated (blue) and experimental pattern (orange) of **1·2H<sub>2</sub>O** (blue).

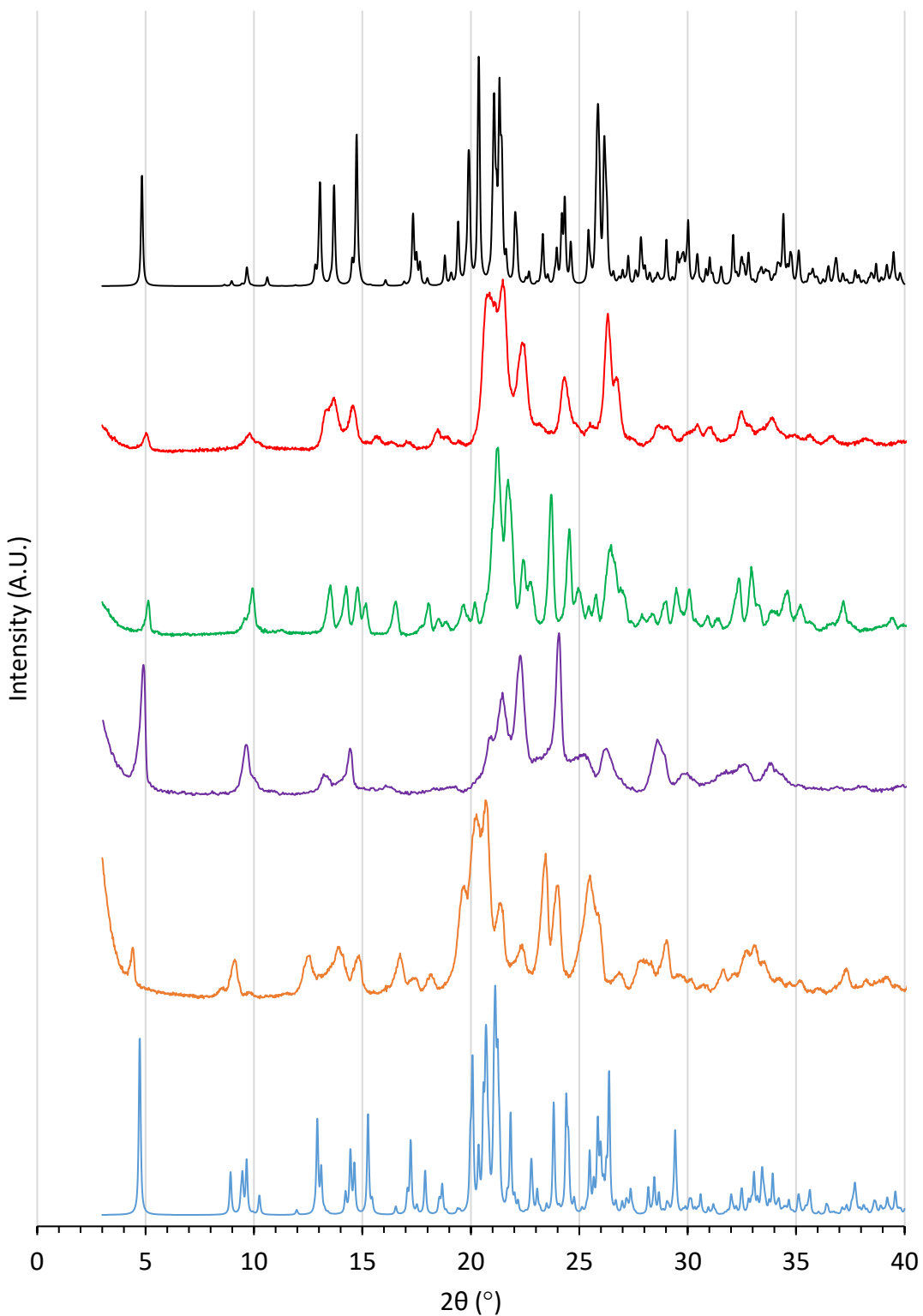


**Figure S 31** Calculated pattern of  $\mathbf{1} \cdot 't\text{PrOH}$  (blue) and experimental patterns of bulk mixed-phase materials isolated from  $'\text{PrOH}$  (orange),  $''\text{PrOH}$  (purple),  $''\text{BuOH}$  (green),  $'t\text{BuOH}$  (red) and a calculated pattern of the dihydrate phase  $\mathbf{1} \cdot 2\text{H}_2\text{O}$  (black). The formulas for these as bulk materials are  $\mathbf{1} \cdot \frac{1}{2}'\text{PrOH} \cdot 2\text{H}_2\text{O}$ ,  $\mathbf{1} \cdot \frac{1}{2}''\text{PrOH} \cdot \text{H}_2\text{O}$ ,  $\mathbf{1} \cdot \frac{1}{3}''\text{BuOH} \cdot 0.5\text{H}_2\text{O}$ ,  $\mathbf{1} \cdot \frac{1}{3}'t\text{BuOH} \cdot 1.66\text{H}_2\text{O}$ .

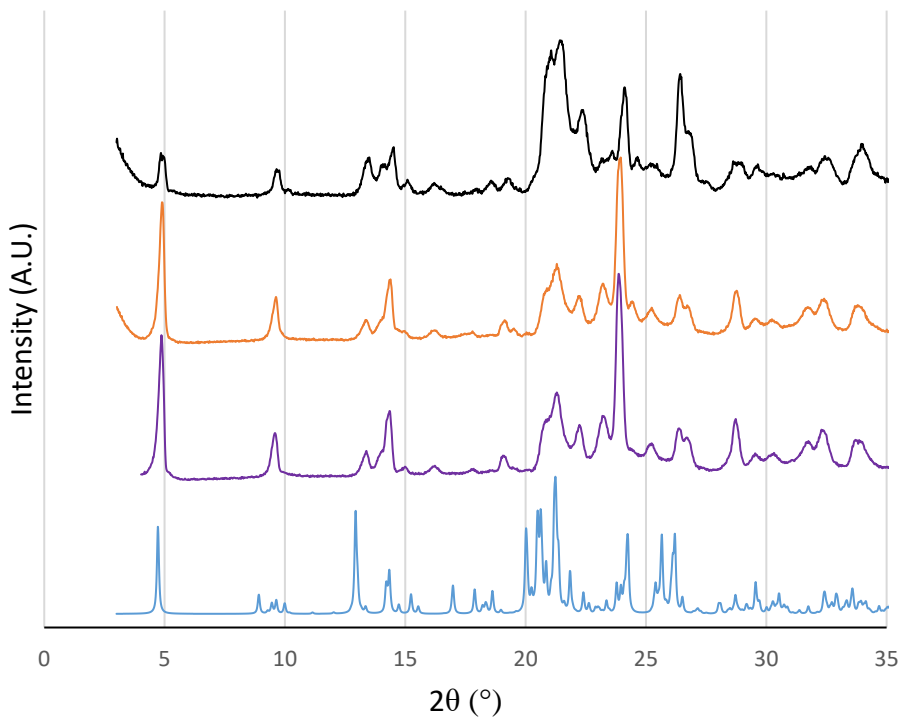


**Figure S 32** Calculated (blue) and experimental patterns of **1·2MeOH** from MeOH-H<sub>2</sub>O solution (purple) reagent grade MeOH solution (purple) and dry MeOH solution (black).

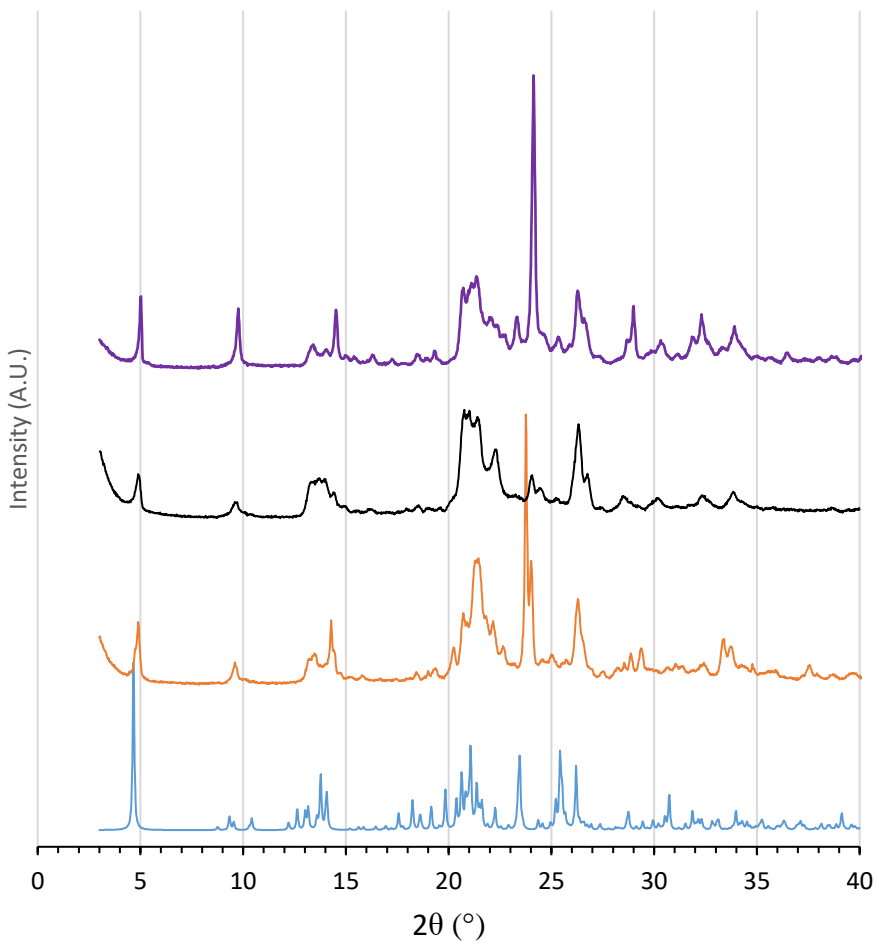


**Figure S 33** Calculated (blue) and experimental patterns of **1**·EtOH·2H<sub>2</sub>O from EtOH-H<sub>2</sub>O solution (orange) reagent grade EtOH solution (black) and dry EtOH solution (purple).

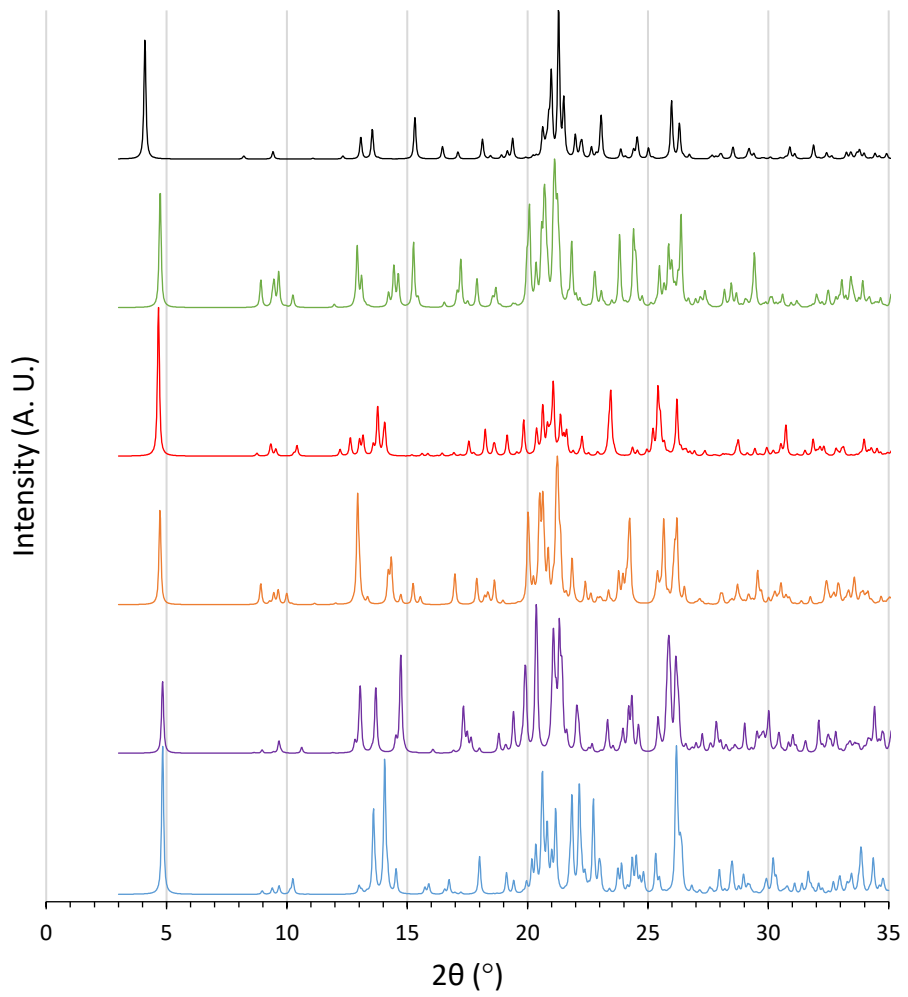


**Figure S 34** Calculated patterns for **1**·3H<sub>2</sub>O (blue), **1**·2H<sub>2</sub>O (purple), **1**·2MeOH (orange), **1**·EtOH·2H<sub>2</sub>O (red), **1**·iPrOH (green), **1**·2DMSO (black).

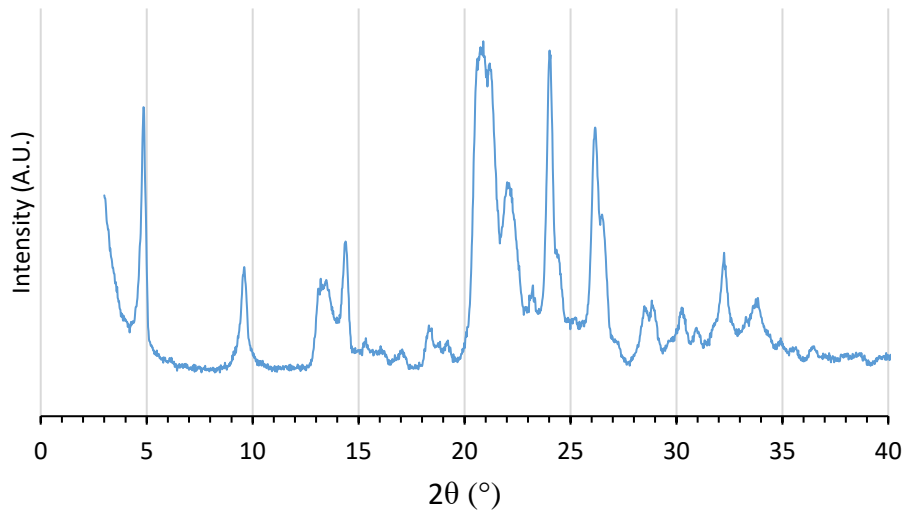


**Figure S 35** Experimental pattern for the multi-alcohol solid obtained from the reaction in equi-volume MeOH, EtOH, *i*PrOH and *t*BuOH solution.

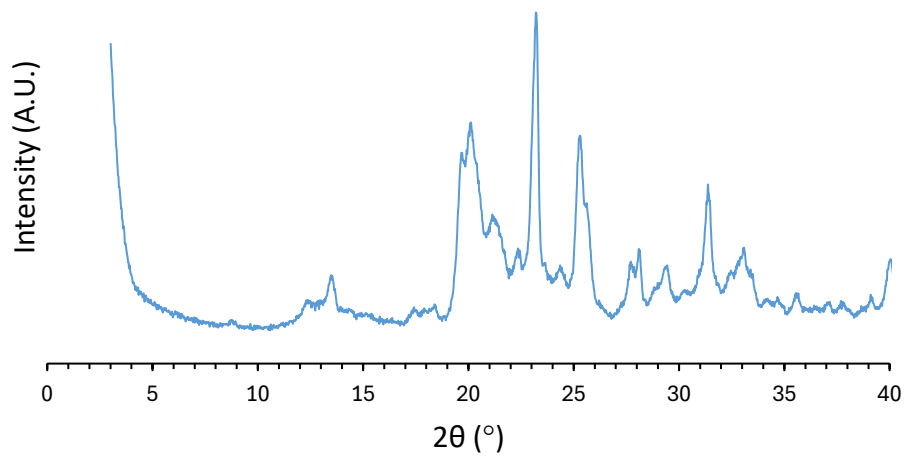


**Figure S 36** Experimental pattern for the multi-alcohol solid obtained from the reaction in equi-volume MeOH, EtOH, *n*PrOH and *n*BuOH solution.

## 6. TG-DSC Data

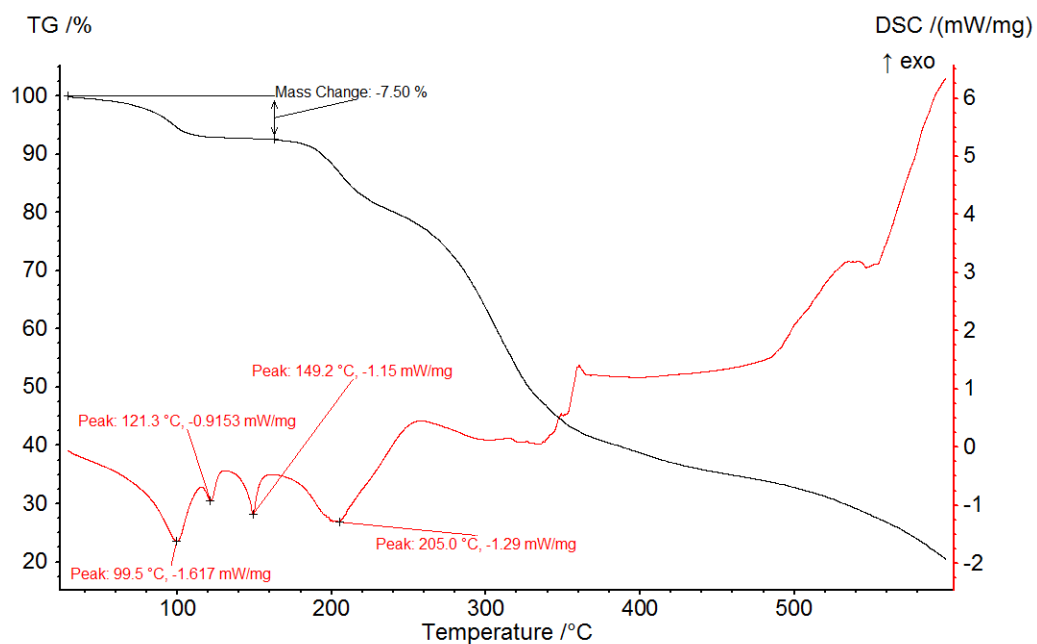


**Figure S 37** The TG-DSC trace of **1·3H<sub>2</sub>O** under an atmosphere of 10% O<sub>2</sub> in N<sub>2</sub>. The TG data is shown in black and the DSC data is shown in red.



**Figure S 38** Image of the orange liquid obtained (**1-IL**) from heating **1·3H<sub>2</sub>O** to 150 °C.

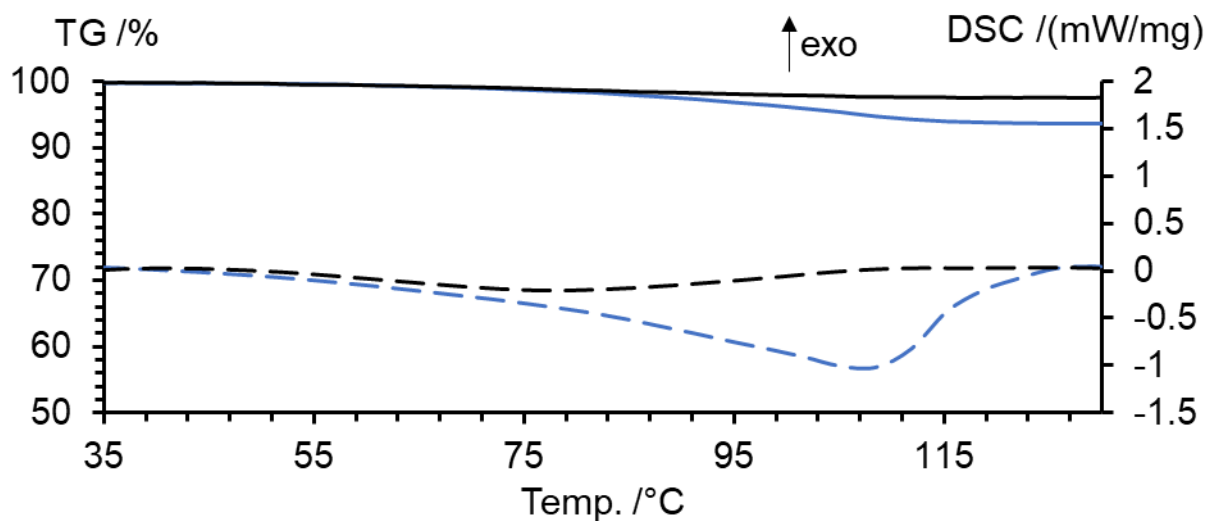


**Figure S 39** A comparison of the TG-DSC traces of **1·3H<sub>2</sub>O** (blue) and **1·IL** (black) after 3 weeks of exposure to the atmosphere. The TG data is shown in solid lines and the DSC data is shown in dashed lines.

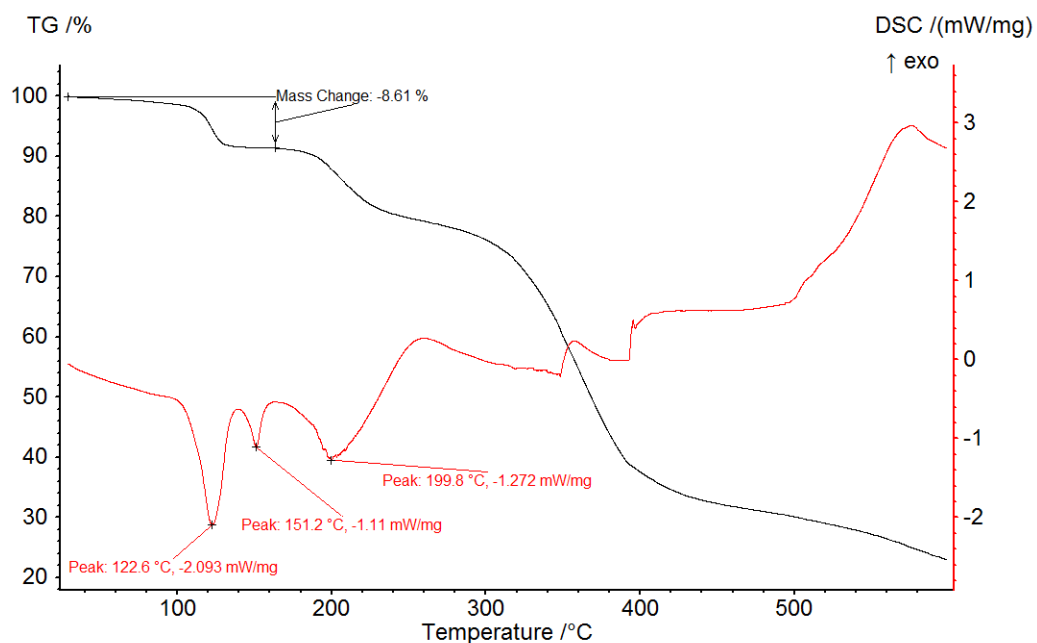


**Figure S 40** The TG-DSC trace of **1·2MeOH** under an atmosphere of 10% O<sub>2</sub> in N<sub>2</sub>. The TG trace is shown in black and the DSC trace is shown in red.

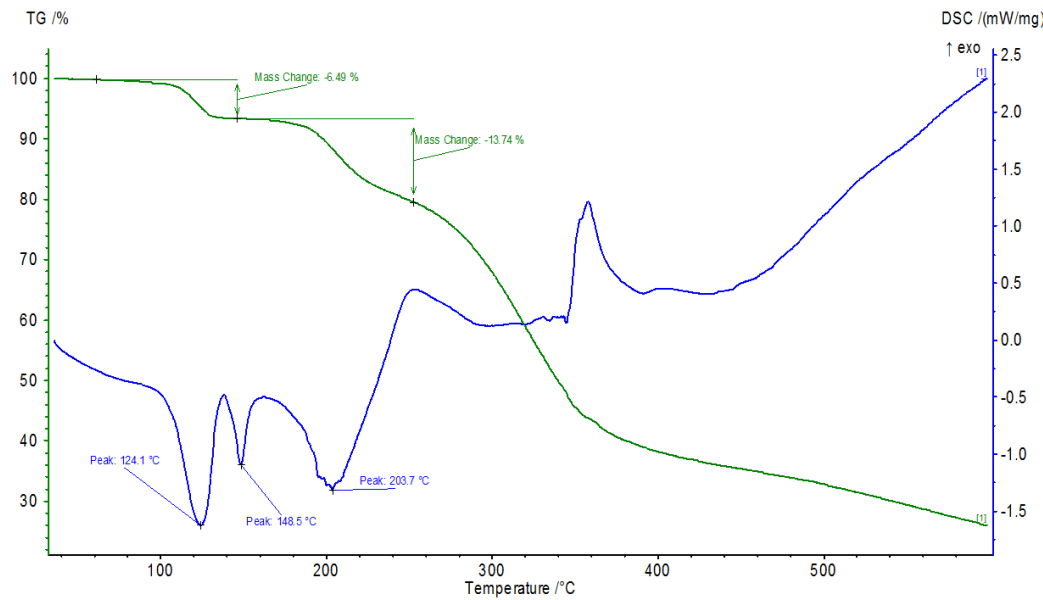


**Figure S 41** The TG-DSC trace of the bulk material from the reaction in ethanol (**1**·EtOH·2H<sub>2</sub>O) under an atmosphere of 10% O<sub>2</sub> in N<sub>2</sub>. The TG trace is shown in green and the DSC trace is shown in blue.

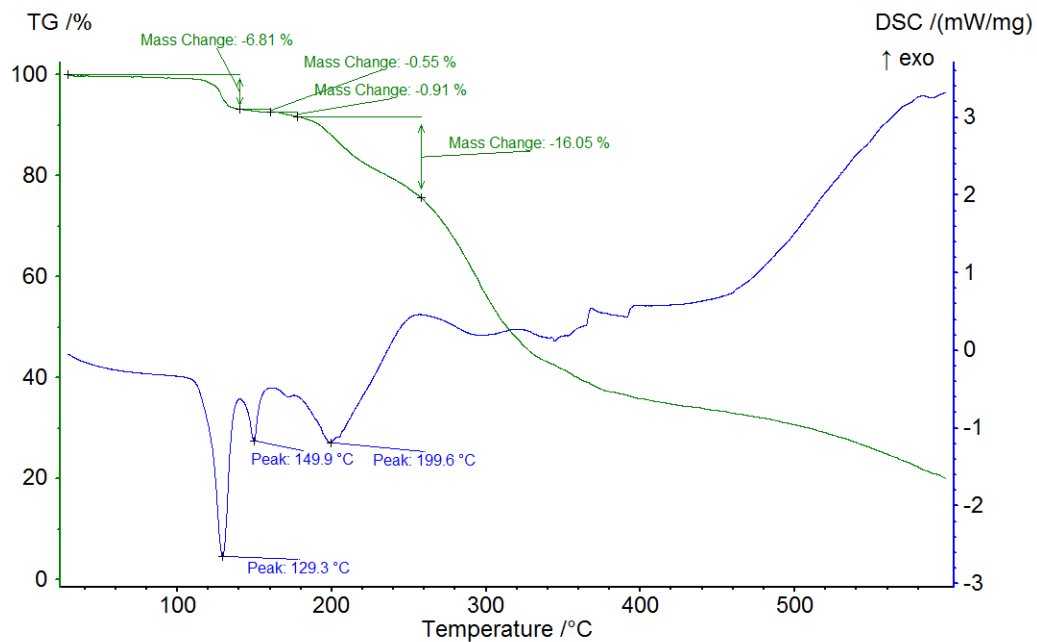


**Figure S 42** The TG-DSC trace of the bulk material from the reaction in ethanol-water (**1**·½EtOH·2H<sub>2</sub>O) under an atmosphere of 10% O<sub>2</sub> in N<sub>2</sub>. The TG trace is shown in green and the DSC trace is shown in blue.

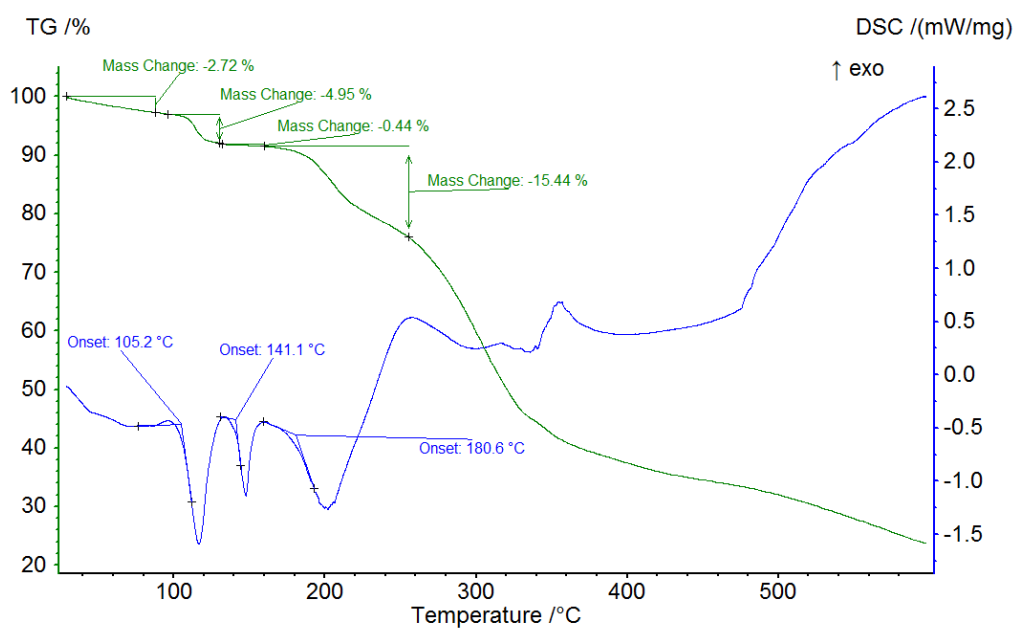


**Figure S 43** The TG-DSC trace of the bulk material isolated from the reaction in isopropanol (**1**·½/PrOH·2H<sub>2</sub>O) under an atmosphere of 10% O<sub>2</sub> in N<sub>2</sub>. The TG trace is shown in green and the DSC trace is shown in blue.

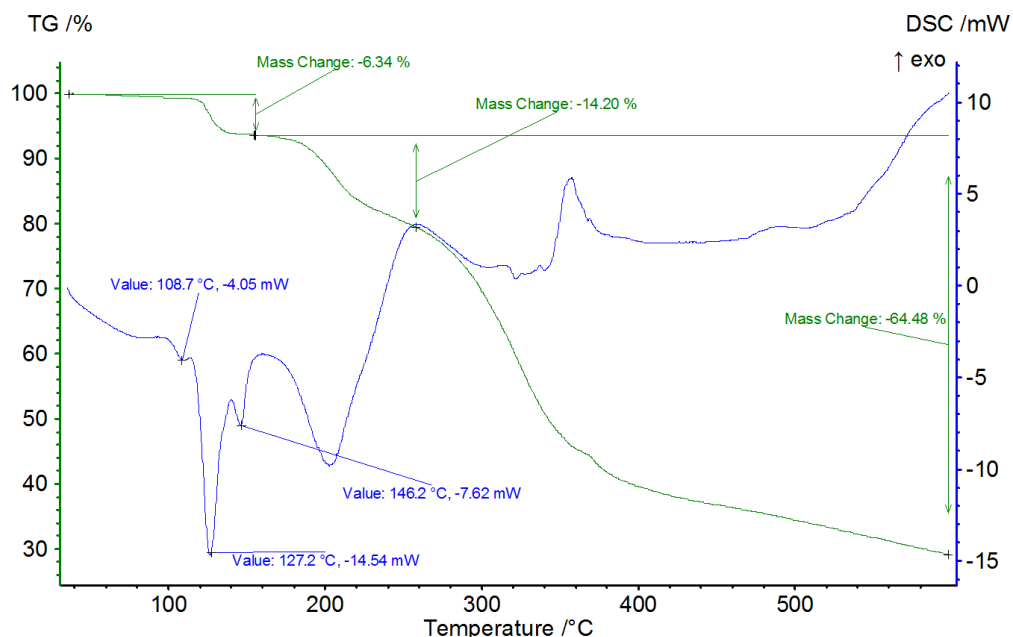


**Figure S 44** The TG-DSC trace of the bulk material isolated from the reaction in *n*-propanol under an atmosphere of 10% O<sub>2</sub> in N<sub>2</sub>. The TG trace is shown in green and the DSC trace is shown in blue.

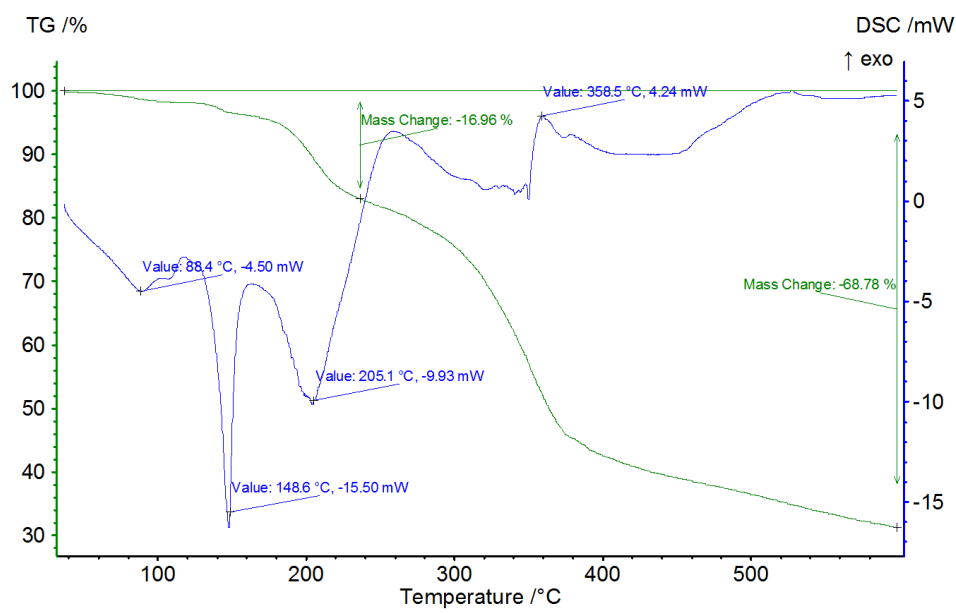


**Figure S 45** The TG-DSC trace of the material isolated from the reaction in *n*-butanol (**1**· $\frac{1}{3}$ <sup>*n*</sup>BuOH·½H<sub>2</sub>O) under an atmosphere of 10% O<sub>2</sub> in N<sub>2</sub>. The TG trace is shown in green and the DSC trace is shown in blue.

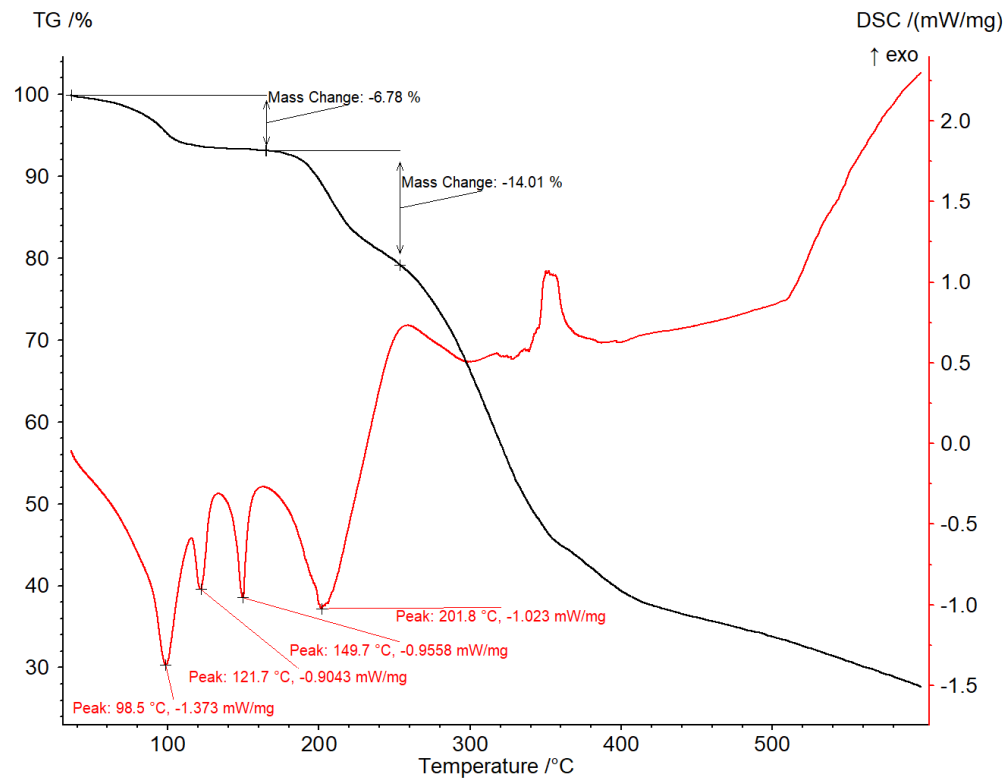


**Figure S 46** The TG-DSC trace of the bulk material isolated from the reaction in *tert*-butanol (**1**· $\frac{1}{3}$ <sup>*t*</sup>BuOH·1.66H<sub>2</sub>O) under an atmosphere of 10% O<sub>2</sub> in N<sub>2</sub>. The TG trace is shown in black and the DSC trace is shown in red.

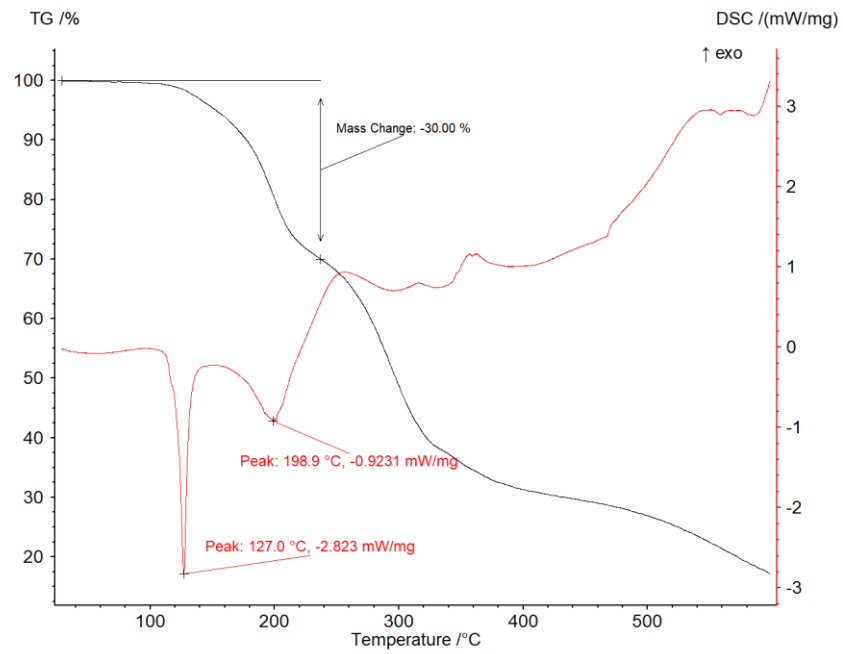


**Figure S 47** The TG-DSC trace of **1·2DMSO** under an atmosphere of 10% O<sub>2</sub> in N<sub>2</sub>. The TG data is shown in black and the DSC data is shown in red.

**Table S 4** Data for solvate loss calculations from bulk as-synthesised compounds.

Compound	Formula	Empirical formula	Molecular Mass (g·mol <sup>-1</sup> )
<b>1·3H<sub>2</sub>O</b>	(dcfn) <sub>2</sub> (H <sub>2</sub> pn)(H <sub>2</sub> O) <sub>3</sub> (C <sub>14</sub> H <sub>10</sub> Cl <sub>2</sub> N <sub>1</sub> O <sub>2</sub> ) <sub>2</sub> (C <sub>3</sub> H <sub>12</sub> N <sub>2</sub> )(H <sub>2</sub> O) <sub>3</sub>	C <sub>31</sub> H <sub>38</sub> Cl <sub>4</sub> N <sub>4</sub> O <sub>7</sub>	720.40
<b>1·2DMSO</b>	(dcfn) <sub>2</sub> (H <sub>2</sub> pn)(DMSO) <sub>2</sub> (C <sub>14</sub> H <sub>10</sub> Cl <sub>2</sub> N <sub>1</sub> O <sub>2</sub> ) <sub>2</sub> (C <sub>3</sub> H <sub>12</sub> N <sub>2</sub> )(C <sub>2</sub> H <sub>6</sub> SO) <sub>2</sub>	C <sub>35</sub> H <sub>44</sub> Cl <sub>4</sub> N <sub>4</sub> O <sub>6</sub> S <sub>2</sub>	822.60
<b>1·2MeOH</b>	(dcfn) <sub>2</sub> (H <sub>2</sub> pn)(MeOH) <sub>2</sub> (C <sub>14</sub> H <sub>10</sub> Cl <sub>2</sub> N <sub>1</sub> O <sub>2</sub> ) <sub>2</sub> (C <sub>3</sub> H <sub>12</sub> N <sub>2</sub> )(CH <sub>4</sub> O) <sub>2</sub>	C <sub>33</sub> H <sub>40</sub> Cl <sub>4</sub> N <sub>4</sub> O <sub>6</sub>	730.43
<b>1·EtOH·2H<sub>2</sub>O</b>	(dcfn) <sub>2</sub> (H <sub>2</sub> pn)(EtOH)(H <sub>2</sub> O) <sub>2</sub> (C <sub>14</sub> H <sub>10</sub> Cl <sub>2</sub> N <sub>1</sub> O <sub>2</sub> ) <sub>2</sub> (C <sub>3</sub> H <sub>12</sub> N <sub>2</sub> )(C <sub>2</sub> H <sub>6</sub> O)(H <sub>2</sub> O) <sub>2</sub>	C <sub>33</sub> H <sub>42</sub> Cl <sub>4</sub> N <sub>4</sub> O <sub>7</sub>	748.45
<b>1·½<i>i</i>EtOH·2H<sub>2</sub>O</b>	(dcfn) <sub>2</sub> (H <sub>2</sub> pn)(EtOH) <sub>0.5</sub> (H <sub>2</sub> O) <sub>2</sub> (C <sub>14</sub> H <sub>10</sub> Cl <sub>2</sub> N <sub>1</sub> O <sub>2</sub> ) <sub>2</sub> (C <sub>3</sub> H <sub>12</sub> N <sub>2</sub> )(C <sub>2</sub> H <sub>6</sub> O) <sub>0.5</sub> (H <sub>2</sub> O) <sub>2</sub>	C <sub>32</sub> H <sub>39</sub> Cl <sub>4</sub> N <sub>4</sub> O <sub>6.5</sub>	725.42
<b>1·½<i>i</i>PrOH·2H<sub>2</sub>O</b>	(dcfn) <sub>2</sub> (H <sub>2</sub> pn)( <i>i</i> PrOH) <sub>0.5</sub> (H <sub>2</sub> O) <sub>2</sub> (C <sub>14</sub> H <sub>10</sub> Cl <sub>2</sub> N <sub>1</sub> O <sub>2</sub> ) <sub>2</sub> (C <sub>3</sub> H <sub>12</sub> N <sub>2</sub> )(C <sub>3</sub> H <sub>8</sub> O) <sub>0.5</sub> (H <sub>2</sub> O) <sub>2</sub>	C <sub>32.5</sub> H <sub>40</sub> Cl <sub>4</sub> N <sub>4</sub> O <sub>6.5</sub>	732.43
<b>1·2H<sub>2</sub>O</b>	(dcfn) <sub>2</sub> (H <sub>2</sub> pn)(H <sub>2</sub> O) <sub>2</sub> (C <sub>14</sub> H <sub>10</sub> Cl <sub>2</sub> N <sub>1</sub> O <sub>2</sub> ) <sub>2</sub> (C <sub>3</sub> H <sub>12</sub> N <sub>2</sub> )(H <sub>2</sub> O) <sub>2</sub>	C <sub>31</sub> H <sub>36</sub> Cl <sub>4</sub> N <sub>4</sub> O <sub>6</sub>	702.38
<b>1·½<sup>n</sup>PrOH·½H<sub>2</sub>O</b>	(dcfn) <sub>2</sub> (H <sub>2</sub> pn)( <sup>n</sup> PrOH) <sub>0.5</sub> (H <sub>2</sub> O) (C <sub>14</sub> H <sub>10</sub> Cl <sub>2</sub> N <sub>1</sub> O <sub>2</sub> ) <sub>2</sub> (C <sub>3</sub> H <sub>12</sub> N <sub>2</sub> )(C <sub>3</sub> H <sub>8</sub> O) <sub>0.5</sub> (H <sub>2</sub> O)	C <sub>32.5</sub> H <sub>38</sub> Cl <sub>4</sub> N <sub>4</sub> O <sub>5.5</sub>	714.42
<b>1·½<sup>n</sup>BuOH·½H<sub>2</sub>O</b>	(dcfn) <sub>2</sub> (H <sub>2</sub> pn)( <sup>n</sup> BuOH) <sub>0.33</sub> (H <sub>2</sub> O) <sub>0.5</sub> (C <sub>14</sub> H <sub>10</sub> Cl <sub>2</sub> N <sub>1</sub> O <sub>2</sub> ) <sub>2</sub> (C <sub>3</sub> H <sub>12</sub> N <sub>2</sub> )(C <sub>4</sub> H <sub>10</sub> O) <sub>0.33</sub> (H <sub>2</sub> O) <sub>0.5</sub>	C <sub>32.33</sub> H <sub>36.33</sub> Cl <sub>4</sub> N <sub>4</sub> O <sub>4.83</sub>	700.06
<b>1·½<sup>t</sup>BuOH·1.66H<sub>2</sub>O</b>	(dcfn) <sub>2</sub> (H <sub>2</sub> pn)( <sup>t</sup> BuOH) <sub>0.33</sub> (H <sub>2</sub> O) <sub>1.66</sub> (C <sub>14</sub> H <sub>10</sub> Cl <sub>2</sub> N <sub>1</sub> O <sub>2</sub> ) <sub>2</sub> (C <sub>3</sub> H <sub>12</sub> N <sub>2</sub> )(C <sub>4</sub> H <sub>10</sub> O) <sub>0.33</sub> (H <sub>2</sub> O) <sub>1.66</sub>	C <sub>32.33</sub> H <sub>38.66</sub> Cl <sub>4</sub> N <sub>4</sub> O <sub>6</sub>	721.08
<b>1</b>	(dcfn) <sub>2</sub> (pnH <sub>2</sub> ) (C <sub>14</sub> H <sub>10</sub> Cl <sub>2</sub> N <sub>1</sub> O <sub>2</sub> ) <sub>2</sub> (C <sub>3</sub> H <sub>12</sub> N <sub>2</sub> )	C <sub>31</sub> H <sub>32</sub> Cl <sub>4</sub> N <sub>4</sub> O <sub>4</sub>	666.35

Calculation of solvate loss:

**1·3H<sub>2</sub>O:**  $(720.40 - 666.35) / 720.40 = 7.5\%$ . Observed 7.5%.

**1·2DMSO:**  $(822.60 - 666.35) / 822.60 = 18.9\%$ . Observed with melting of the compound and in combination with loss due to the thermal reaction that releases water. Mass loss for these combined events was 30%

**1·2MeOH:**  $(730.43 - 666.35) / 730.43 = 8.8\%$ . Observed 8.6%.

**1·EtOH·2H<sub>2</sub>O:**  $(748.45 - 666.35) / 748.45 = 10.9\%$ . Observed 6.8%.

**1·½EtOH·2H<sub>2</sub>O:**  $(725.42 - 666.35) / 725.42 = 8.1\%$ . Observed 7.5%.

**1·½/PrOH·2H<sub>2</sub>O:**  $(732.43 - 666.35) / 732.43 = 9.0\%$ . Observed 8.1%.

**1·2H<sub>2</sub>O:**  $(702.38 - 666.35) / 702.38 = 5.1\%$ . Observed 5.1%.

**1·½/*n*PrOH·H<sub>2</sub>O:**  $(714.42 - 666.35) / 714.42 = 6.7\%$ . Observed 6.3%.

**1·½/*n*BuOH·½H<sub>2</sub>O:**  $(700.06 - 666.35) / 700.42 = 4.9\%$ . Observed 5.9%.

**1·½/*t*BuOH·1.66H<sub>2</sub>O:**  $(721.08 - 666.35) / 721.08 = 7.6\%$ . Observed 6.8%.

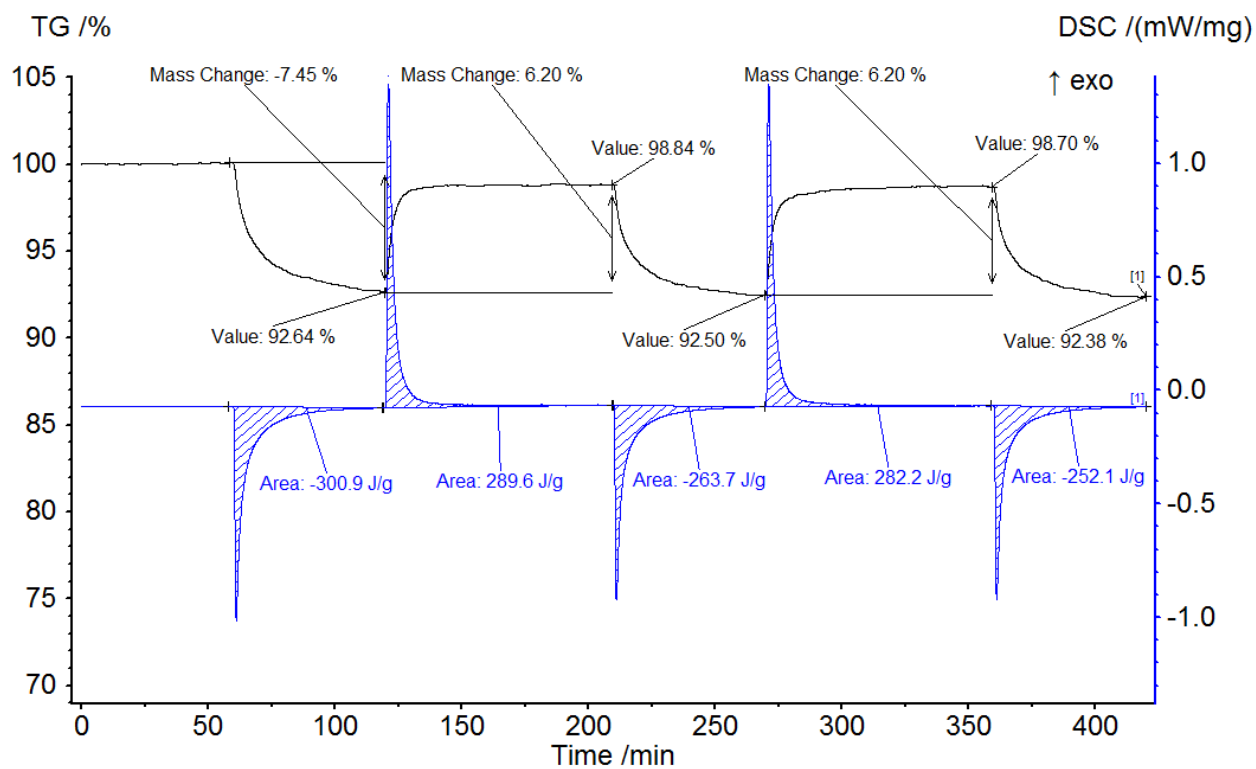


**Figure S 48** This is Figure 13 in the manuscript with all the calorific data from cycling **1**· $3\text{H}_2\text{O}$  directly between 50% RH and 0% RH (50→0→50→0→50→0). The TG data is shown in black and the DSC data is shown in blue.

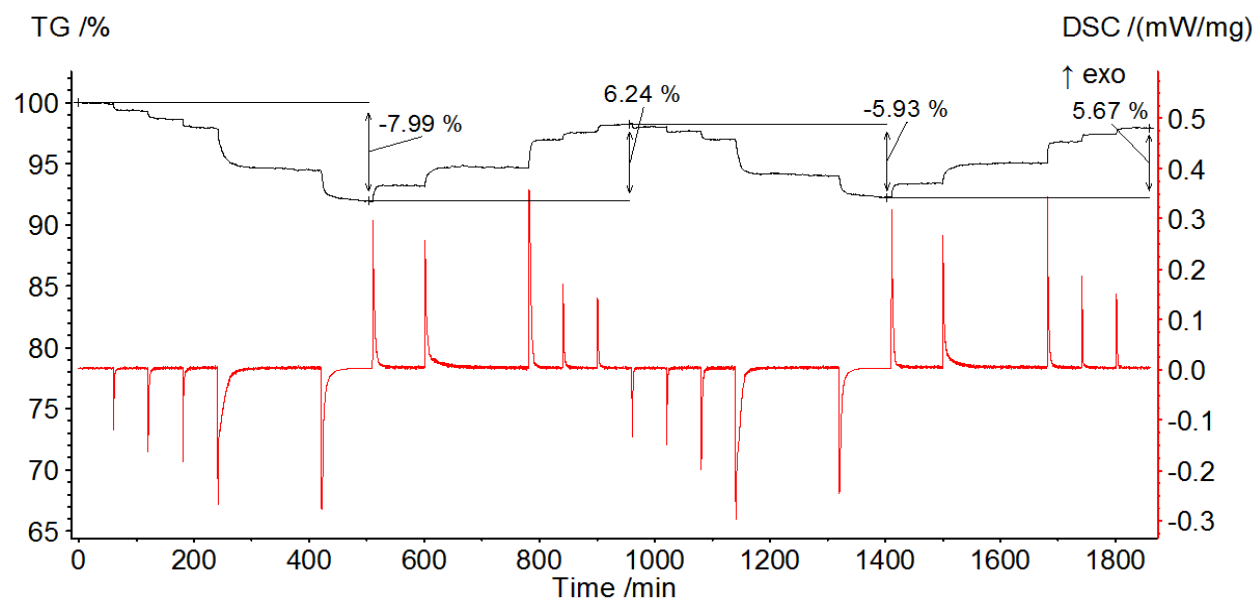


**Figure S 49** A desorption-adsorption-desorption-adsorption TG-DSC trace of **1**· $3\text{H}_2\text{O}$  with respect to time with 10% increments in RH (50→0→50→0→50). The TG data is shown in black and the DSC data is shown in red.

## 7. ESI Mass Spectrometry

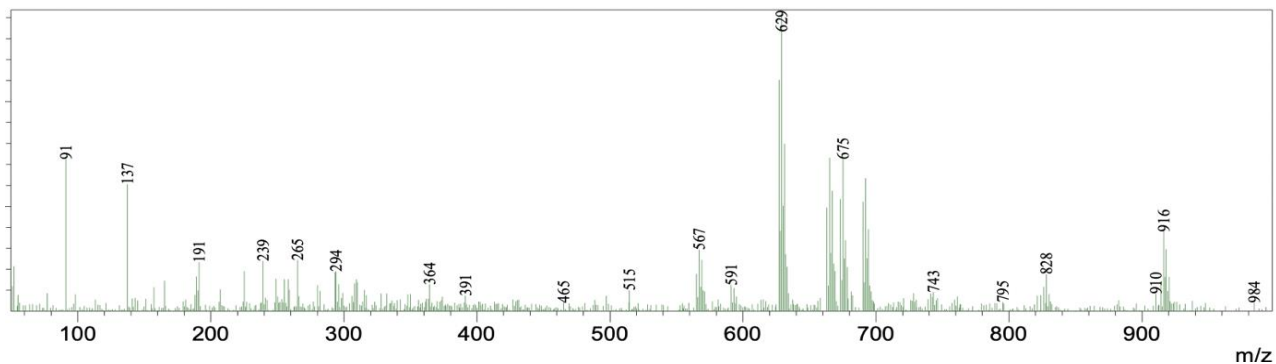


**Figure S 50** Low resolution ESI negative ion spectrum of the crude product from heating **1·3H<sub>2</sub>O** to 200 °C and holding for 10 minutes. The base peak is 629 *m/z*. Chemical Formula: C<sub>31</sub>H<sub>27</sub>Cl<sub>4</sub>N<sub>4</sub>O<sub>2</sub><sup>-</sup> *m/z*: 629.09 (100.0%).